Hendry, K., & Brzezinski, M. (2014). Using silicon isotopes to understand the role of the Southern Ocean in modern and ancient biogeochemistry and climate. Quaternary Science Reviews, 89, 13-26. 10.1016/j.quascirev.2014.01.019

Using silicon isotopes to understand the role of the Southern Ocean in modern and ancient biogeochemistry and climate

Katharine R. Hendry[1,2#] & Mark A. Brzezinski[3,4]

[1] School of Earth and Ocean Sciences, Cardiff University, Park Place, Cardiff CF10 3AT, UK

[2] School of Earth Sciences, Bristol University, Wills Memorial Building, Queen's Road, Bristol BS8 1RJ, UK

[3] Department of Ecology Evolution and Marine Biology and the Marine Sciences Institute, University of California, Santa Barbara, CA 93106-6150, USA

[4]Marine Science Institute, University of California, Santa Barbara, 93106-6150, USA

 # Corresponding author, K.Hendry@bristol.ac.uk, Tel: +44 (0)117 954 5400

Abstract

The growth of siliceous phytoplankton, mainly diatoms, in the Southern Ocean influences the preformed nutrient inventory in the ocean on a global scale. Silicic acid use by diatoms and deep circulation combine to trap dissolved Si in the Southern Ocean resulting in high levels of silica production and expansive diatom oozes in Southern Ocean sediments. The analysis of the silicon isotope composition of biogenic silica, or opal, and dissolved silicic acid provide insight into the operation of the global marine silicon cycle and the role played by the Southern Ocean in nutrient supply and carbon drawdown, both in the modern and in the past. Silicon isotope studies of diatoms have provided insight into the history of silica production in surface waters, while the analysis of spicules from deep sea sponges has defined both the spatial and the temporal variability of silicic acid concentrations in the water column; together these – and other

- proxies reveal variations in the northward flow of Southern Ocean intermediate and mode waters and how changes in Southern Ocean productivity altered their preformed nutrient content. We present a new hypothesis – the "Silicic Acid Ventilation Hypothesis" (SAVH) – to explain the geographical variation of opal-based proxy records, in particular the contrasting patterns of opal burial change found in the low and high latitudes. By understanding the silicon isotope systematics of opal and silicic acid in the modern, we will be able to use opal-based proxies to reconstruct past changes in the Southern Ocean and so investigate its role in global carbon cycling and climate.

Keywords: silicon isotope, silicic acid, opal, diatom

1. Introduction

1.1 Background and motivation

The Southern Ocean plays a central role in governing the inventory of preformed nutrients and carbon storage in the global ocean (Marinov et al., 2008; Marinov et al., 2006). Of particular interest is the role of Southern Ocean circulation and biogeochemistry as a major control on the global distribution of the dissolved silicon - silicic acid or $Si(OH)_4$ – and as the single largest locus of modern opal deposition on the seafloor (Cortese et al., 2004; Figure 1). The formation and burial of biogenic opal, amorphous silica, is the most important sink of $Si(OH)_4$ in the modern oceans, and is formed predominantly by diatoms, a diverse group of photosynthetic protists from the Class Bacillariophyceae. Diatoms have an absolute requirement for $Si(OH)_4$ and have evolved mechanisms for efficient Si uptake and metabolism (Martin-Jezequel et al., 2003). $Si(OH)_4$ uptake by diatoms severely depletes dissolved Si from surface waters (Falkowski et al., 2004). As such, diatoms rely on upwelled waters with elevated $Si(OH)_4$, thriving in ecosystems such as coastal and open ocean

upwelling zones, areas of deep winter mixing (such as the Southern Ocean frontal zones), and – in the case of some giant diatoms – obtaining their requisite silicon from deep nutriclines in highly stratified waters (Kemp et al., 2006).

Diatoms contribute up to 40% of global marine primary productivity, and approximately half of the opal produced in the euphotic zone is exported to deep waters (Nelson et al., 1995; Tréguer et al., 1995). Approximately 3% of biogenic opal production is preserved in ocean floor sediments as a global average (Nelson et al., 1995), with the remainder remineralized in the water column or at the sediment-water interface (reviewed by Tréguer and De la Rocha, 2013). Although the Southern Ocean is the single largest site of opal deposition (the "opal belt") in the modern ocean (Cortese et al., 2004), opal preservation efficiency in the Southern Ocean is not significantly different from the global average (2-6%; DeMaster, 2002; Nelson et al., 2002; Pondaven et al., 2000) such that the high opal accumulation rates in Southern Ocean sediments is sustained by high rates of opal production rather than high preservation efficiency.

Diatom opal has received significant scrutiny over the past decades as a source of paleoceanographic information. Southern Ocean waters are often too corrosive for the preservation of traditional carbonate proxies, creating substantial interest in using opal as an indicator of past changes in southern component water. Opal accumulation rates, when ^{230}Th-normalised to account for sediment redistribution, provide an important constraint on the productivity and export of diatoms from surface waters into deep waters and sediments (Chase et al., 2003b). ^{231}Pa/^{230}Th ratios in opal-rich regions provide an additional constraint on opal production, versus preservation, due to the affinity of ^{231}Pa for opal (Chase et al., 2002). Given the dependence of diatoms on deep sources of $Si(OH)_4$, ^{230}Th-normalised opal accumulation rates, paired with ^{231}Pa/^{230}Th ratios, have been used as a proxy for wind-driven upwelling in the Southern Ocean (Anderson et al., 2009).

In addition to opal accumulation, there has been an increasing interest in the last twenty years on the use of aspects of opal chemistry as biogeochemical proxies for environmental conditions and productivity, including elemental ratios of occluded trace constituents (Ellwood and Hunter, 1999; Hendry and Rickaby, 2008; Lal et al., 2006) and stable isotopes of Si (De La Rocha et al., 1997; De La Rocha et al., 1998), O (Leng and Sloane, 2008; Shemesh, 1995), and more recently Zn (Andersen et al., 2011; Hendry and Andersen, 2013). One of the widest used applications is that of Si isotope analysis of diatom opal as a proxy for silica production. Briefly, there are three naturally occurring stable isotopes of silicon, ^{28}Si (~92 atom %), ^{29}Si (~5 atom %) and ^{30}Si (~3 atom %), and the silicon isotope composition of a material is denoted by $\delta^{30}Si$, where:

$$\delta^{30}Si = [(^{30}Si/^{28}Si)_{sample}/(^{30}Si/^{28}Si)_{standard\text{-}NBS28} - 1] \times 1000 \quad (1)$$

De La Rocha and co-workers first reported on the fractionation of isotopes of Si by diatoms using laboratory cultures (De La Rocha et al., 1997). That work indicated that diatoms have a constant fractionation factor (ε) favouring the lighter isotope ^{28}Si over ^{30}Si by ~1.1 ‰, with similar results achieved a few years later in further culture studies (Milligan et al., 2004) and field observations of water column diatoms (Fripiat et al., 2012; Fripiat et al., 2011; Varela et al., 2004), but see Sutton et al (2013) for evidence for possible interspecific variation in ε (see below). Hence, as $Si(OH)_4$ utilization increases, both dissolved silicic acid and the opal produced from it become progressively enriched in the heavier isotopes of Si, such that the silicon isotopic composition of diatom opal extracted from dated sediment cores can be used as a measure of past surface ocean Si utilization. These concepts were first applied to downcore records of diatom $\delta^{30}Si$ from the Southern Ocean (De La Rocha et al., 1998). This progressive fractionation can be modelled as a Rayleigh-type closed distillation process, or a steady state open system, assuming a constant value of ε and a known starting

isotopic composition of the nutrient substrate (De La Rocha et al., 1997; Varela et al., 2004).

The aim of this review is to bring together advances in oceanic silicon isotope studies with a focus on the role of Southern Ocean circulation and productivity in controlling the global distribution of $Si(OH)_4$ and the contribution of diatoms to global marine productivity. We will explore controls on Si isotope distribution deduced from models of modern oceanic $\delta^{30}Si(OH)_4$ distributions, the application of Si isotopes to paleoceanographic studies of Earth's climate, using the Silicic Acid Leakage Hypothesis (SALH) as a case study, and the future of opal-based multi-proxy approaches in paleoceanography.

2. Silicon isotopes as a silica production proxy

2.1. Culture experiments on diatoms

Since the original studies of De la Rocha et al. (1997) and Milligan et al. (2004), there was a considerable gap before further laboratory culture studies were carried out, which ended only recently with the publication of new culture experiments by Sutton et al. (2013). These culture experiments used the same species as the original studies (*Thalassiosira weissflogii* and *T. pseudonana*, De La Rocha et al., 1997; Milligan et al., 2004), and some Southern Ocean species that had not been previously studied (*Porosira glacilis, T. antarctica, T. nordenskioeldii, Fragilariopsis kerguelensis, Chaeotceros brevis*). Most of the results were consistent with the original findings (Figure 2), supporting the paradigm that diatom ε has a value of -1.1 ‰ within experimental uncertainty. However, there were some discrepancies between the different studies for different strains of the same species, *T. weissflogii*. Furthermore, two polar species had significantly different fractionation factors: *F. kerguelensis* showed a ε value of -0.54 ‰ (mean for two strains) and *C. brevis* showed a ε value of -2.09 ‰ (Sutton et al., 2013). Two major questions arising from these studies are: Do the results of culture experiments capture the range of fractionation by diatoms in the

natural environment? And, is interspecific variation in ε, as represented by the extreme value for *C. brevis*, detectable in nature?

2.2. Proxy verification: Core top calibrations of diatoms

2.2.1. Cleaning methods

An important aspect of paleoceanographic applications of opal composition is the effective cleaning of frustules to remove clays and fragments of other biogenic opal producers (radiolarians, sponge spicules). Heavy liquid separation has been used routinely for opal analysis for over twenty years, but there are numerous different approaches for further physical and chemical cleaning of the opal prior to analysis (Ellwood and Hunter, 1999; Hendry and Rickaby, 2008; Lal et al., 2006; Shemesh, 1989). Most studies of diatom Si isotopes have employed variants on these more traditional methods. Most recently, a microfiltration method originally designed to separate different species of coccoliths from sediments (Minoletti et al., 2009) has recently been adapted for the cleaning and separation of different size fractions of opal (Egan et al., 2012). The gentle sonication of the samples limits the potential for frustule fragmentation and thus mechanical loss of material. The studies show that size fractions for core tops in the Southern Ocean between 2-20 μm contain only clean diatom opal and yield reproducible δ^{30}Si values. Fractions below and above this range show $\Delta\delta^{30}$Si offsets: <2 μm contain unidentifiable fragments whereas fractions >20 μm contain identifiable fragments of sponge spicules and radiolarians.

There are some potential issues relating to size fractionation of opal samples. Firstly, although the microfiltration method is designed to limit the fragmentation and loss of material, it is still inevitable that material will be lost during the heavy liquid separation stage, any further filtration stages and during chemical cleaning. Secondly, selective loss of more fragile frustules, and size selection of different species, may both reduce apparent variability and introduce a bias into the measurement, for example, towards species that grow at a

149 particular time of year or a particular ambient $Si(OH)_4$ condition. However, the few studies
150 that have been carried out on hand-picked individual frustules of particular species have
151 shown little offset with bulk opal $\delta^{30}Si$ values (e.g. Hendry et al., in press).

152 *2.2.2. Core top calibration results*

153 As alluded to above, one key point to address is whether the opal $\delta^{30}Si$ signal from
154 diatoms in the upper parts of the water column is preserved with fidelity in the sediments. To
155 address this Egan et al. (2012) carried out the first core top calibration of diatom $\delta^{30}Si$ using
156 the microfiltration method. The authors found a good correspondence between the core top
157 diatom $\delta^{30}Si$ from the 2-20 μm size fraction and the minimum annual $Si(OH)_4$ in the
158 overlying surface waters, which, assuming the same initial $Si(OH)_4$ concentration everywhere
159 at the end of winter should reflect the extent of $Si(OH)_4$ depletion. This result suggests that
160 the sedimentary signal reflects the cumulative seasonal drawdown of $Si(OH)_4$ supporting the
161 use of $\delta^{30}Si$ as a production proxy (Egan et al., 2012). Moreover, these data imply that species
162 composition does not impact the $\delta^{30}Si$, once the opal from radiolarians and sponge spicules
163 has been removed. The calculated ε values from the core tops appear to be greater when
164 modelled at steady state from a single source of water (Figure 2). However, the core top
165 results are compatible with an ε value of -1.1 ‰ if fractionation occurs from waters with a
166 $\delta^{30}Si(OH)_4$ composition that lies on a mixing line representing a varying mixture of
167 isotopically heavy surface water and lighter deep water in the Southern Ocean (Egan et al.,
168 2012).

169 ***2.3. Field estimates of the Si fractionation factor***

170 Field estimates of the fractionation factor ε have been made using either the gradient
171 in the isotopic composition of silicic acid across the nutricline, or from the difference between
172 the isotopic composition of co-located samples of biogenic silica and dissolved silicon.

Nutrient and isotope profiles can be used to estimate isotope fractionation using either an open system model (continuous delivery of Si into the euphotic zone) or a closed system model (assuming one isolated pulse of Si delivered into the euphotic zone followed by closed system dynamics) depending on the nature of the vertical nutrient supply. These models are described by the following equations:

$$\text{Open: } \delta^{30}Si(OH)_{4observed} = \delta^{30}Si(OH)_{4initial} - \varepsilon^* (1 - f) \quad (2a)$$

$$\text{Closed: } \delta^{30}Si(OH)_{4observed} = \delta^{30}Si(OH)_{4initial} + \varepsilon^* \ln (f) \quad (2b)$$

where $\delta^{30}Si(OH)_{4observed}$ is the measured $\delta^{30}Si(OH)_4$ in surface waters, $\delta^{30}Si(OH)_{4initial}$ is that of the water mass supplying Si to surface waters and f is the fraction of the supply that remains in surface waters. Simple algebra can be used to show that surface water $\delta^{30}Si(OH)_4$ should be a linear function of $[Si(OH)_4]_{observed} / [Si(OH)_4]_{initial}$ (open) or $\ln[Si(OH)_4]_{observed}$ (closed) with a slope equal to ε (Varela et al. 2004).

In both the open and closed isotope models the $\delta^{30}Si(OH)_4$ of waters ventilating to the surface is required. Uncertainty in this value has led to considerable variations in estimates of ε (Reynolds et al., 2006) inspiring efforts to better understand $\delta^{30}Si(OH)_4$ distributions in subsurface waters.

In principle, ε can also be estimated from the difference between $\delta^{30}Si$ of opal and $\delta^{30}Si(OH)_4$, a parameter denoted by $\Delta\delta^{30}Si$ (Cardinal et al., 2005; De La Rocha et al., 2011; Fripiat et al., 2007). Equating $\Delta\delta^{30}Si$ and ε is only approximate due to the influence of vertical mixing of isotopically light $Si(OH)_4$ altering the biologically-driven relationship between $\delta^{30}Si$ of opal and $\delta^{30}Si(OH)_4$.

A summary of the values of ε from field programs is given in Figure 2. The range of estimated fractionation factors reflects both real-world variation in ε and methodological

196 challenges. Often the simple assumptions made when applying isotope models are violated in
197 natural systems. No system is entirely closed or entirely open causing ambiguity in the
198 correct choice of which isotope model to apply with mixing, also biasing $\Delta\delta^{30}Si$ as described
199 above.

200 In polar regions, biological production associated with seasonal sea ice adds
201 additional complexity to silicon isotope dynamics. In the open waters of the Southern Ocean
202 the limited data available suggest that the isotopic composition of opal sinking to depth
203 reflects patterns in the diatom $\delta^{30}Si$ from the mixed layer (Varela et al., 2004; Fripiat et al,.
204 2012). However, within the relatively closed sea-ice environment of the Antarctic Sea-ice
205 Zone, sea-ice diatoms become distinctly heavy (Fripiat et al., 2007). In that study the unique
206 isotopic signature of the sea ice flora was not detected in the bulk opal signal from the open
207 waters; however, Varela et al (unpublished) found a significant positive correlation between
208 the isotopic composition of opal and the percent ice cover in the Canadian Basin of the Arctic
209 Ocean suggesting a significant contribution of sea ice diatoms to the isotopic signature of
210 opal in open water. Given the importance of sea ice dynamics in polar oceans resolving the
211 contribution of the unique sea ice flora to the silicon isotope dynamics remains an outstanding
212 challenge.

213 ***2.4. Other pelagic biogenic opal producers***

214 In addition to diatoms, other organisms produce biogenic opal, including heterotrophic single-
215 celled radiolarians (supergroup Rhizeria) that live throughout the water column,
216 choanoflagellates (family Acanthoecidae) and silicoflagellates. Considerably less work has
217 been carried out on Si isotope fractionation by radiolarians compared to diatoms (for some
218 discussion, see Egan et al., 2012; Hendry et al., in press; Wu et al., 1997) and, currently,
219 nothing is known about Si fractionation by silicoflagellates or choanoflagellates.

220 **3. Silicon Isotopes in Sponge spicules as a silicic acid concentration proxy**

Whilst sponges are generally considered less important than diatoms to the oceanic Si budget, recent studies suggest that they may contribute more than previously thought to the global uptake of $Si(OH)_4$ (Maldonado et al., 2011). Sponges are simple filter feeding benthic animals (Animalia; Porifera), without tissue grade of organisation. Skeletal support is provided by spicules, formed from proteins, carbonate or – in the case of Classes Demospongea and Hexactinellida – opal. Sponge spicule $\delta^{30}Si$, which has a greater range and is isotopically light compared to diatoms (Egan et al., 2012), was first discussed as a potential paleoproxy a decade ago (De La Rocha, 2003). Following on from this study, two Southern Ocean calibration studies were published (Hendry et al., 2010; Wille et al., 2010), which showed the same relationship between fractionation factor (under equilibrium conditions $\varepsilon \sim \Delta\delta^{30}Si$, ranging from -1 to -5 per mil) and $Si(OH)_4$ (Hendry et al., 2011), according to Equation 3 (Hendry & Robinson, 2012):

$$\Delta\delta^{30}Si = -6.54 + \frac{270}{53 + [Si(OH)_4]} \quad (3)$$

The lack of an apparent relationship between $\delta^{30}Si$ in spicules and species or temperature, pH, salinity, etc., suggests that spicules, from different ocean basins, may provide a robust proxy for past bottom water $Si(OH)_4$ concentrations (Figure 3; Hendry & Robinson, 2012). The non-linear relationship between $\Delta\delta^{30}Si$ and $Si(OH)_4$ concentration is likely a result of a uptake rate effect, whereby fractionation involved with uptake processes also becomes enhanced as Si uptake rates increase with concentration (Hendry and Robinson, 2012; Wille et al., 2010).

The ability of isotopes of Si to provide estimates of relative $Si(OH)_4$ depletion in surface waters (diatom $\delta^{30}Si$) together with estimates of the concentration of Si in ventilating waters (sponge $\delta^{30}Si$) makes $\delta^{30}Si$ unique among the paleo nutrient proxies. Knowing both the concentration of $Si(OH)_4$ in upwelled waters and the fraction of that Si supply that is

utilized in surface waters offers the possibility of estimating absolute silica production rates in the past.

4. Challenges and Caveats

4.1. Is there such a thing as a constant fractionation factor?

In order to fully understand the fractionation occurring during the biomineralization of Si, further work needs to be conducted on understanding the biochemical pathways involved in biosilicification. This is challenging as the biochemistry of biosilicification is largely unknown making it difficult to obtain a mechanistic understanding of how Si isotope fractionation arises in both diatoms and sponges. The fractionation of Si isotopes can potentially occur at several stages of the biosilicification process: uptake of $Si(OH)_4$ from seawater; polymerisation of SiO_2 within the Silica Deposition Vesicle (SDV); and efflux of excess Si from the cell. In diatoms, the efflux of Si does not impact ε (Milligan et al., 2004), which suggests that efflux does not discriminate among isotopes of Si.

The cumulative effect of these processes can be modelled for sponges assuming the fractionation occurs in several steps: firstly as the Si is transported into the cell, secondly as the Si is polymerized, and thirdly as Si is lost from the cell. The fractionation process can be expressed mathematically following Milligan et al., 2004:

$$\Delta\delta^{30}Si = \varepsilon_f = \varepsilon_{tI} + (\varepsilon_p - \varepsilon_{tE})\frac{\nu_E}{\nu_I} \quad (4)$$

Where ε_f = the total Si isotopic fractionation factor, ε_{tI} = Si isotopic fractionation associated with transport into the cell, ε_p = Si isotopic fractionation associated with polymerization and ε_{tE} = Si isotopic fractionation associated with transport out of the cell; ν_E = rate of Si efflux and ν_I = rate of Si influx:

267 $$\varepsilon_f = \varepsilon_{tI} + \Delta\varepsilon_p \left\{ 1 - \frac{\dfrac{v_{\max p}}{\left(\dfrac{K_{mp}}{[Si(OH)_4]} \right) + 1}}{\dfrac{v_{\max t}}{\left(\dfrac{v_{\max t} \times K_{mp} / v_{\max p}}{[Si(OH)_4]} \right) + 1}} \right\} \quad (5)$$

268 where $\varepsilon_p = (\varepsilon_p - \varepsilon_{tE})$; K_m are the half saturation constants and v_{max} are the maximum
269 incorporation rates. In the case of sponges, the half saturation constant and maximum
270 incorporation rate for polymerization have been investigated in two sets of experiments and
271 were found to be 46.41 μM and 19.33 μmol h^{-1} g^{-1} (dry weight) based on explants i.e. tissue
272 transferred to laboratory culture (Reincke and Barthel, 1997) or 74 μM and 1.7 μmol h^{-1} g^{-1}
273 (dry weight) based on whole specimens (Maldonado et al,. 2011). The mathematical solution
274 of Eq. 5 produces non-zero values for the fractionation associated with uptake, efflux and
275 deposition (Hendry & Robinson, 2012). Application of a similar model to diatoms is
276 challenging in the case of diatom field studies due to the difficulties in deconvolving apparent
277 changes in ε due to water mass mixing (Egan et al., 2012), species variation (Sutton et al.,
278 2013), or a possible environmental control on diatom ε as there is for sponges (Hendry &
279 Robinson, 2012).

280 There have been recent developments in mixed layer modelling approaches to
281 investigate possible mechanisms behind the apparent variation in diatom ε. Classic Rayleigh
282 or steady state fractionation models, assuming a constant ε and a uniform upwelling water
283 starting composition, fail to capture the range of apparent ε in the modern ocean, or the
284 greater ε estimated from core tops (Egan et al., 2012). However, these can be reconciled in a
285 number of ways: i) modelling uptake from waters with $\delta^{30}Si(OH)_4$ compositions that lie on

mixing lines between different water masses (as discussed above, Egan et al., 2012); ii) modelling mixed layer processes that occur in the Southern Ocean to take into account higher dissolution rates relative to opal production, and greater supply of $Si(OH)_4$ relative to the uptake by diatoms (Fripiat et al., 2012).

4.2. Alteration of the production signal by fractionation during silica dissolution

One of the most significant outstanding questions in understanding the marine silicon cycle, and the role of the Southern Ocean in the distribution of $Si(OH)_4$ and silicon isotopes, is the impact of dissolution of biogenic opal on apparent isotopic fractionation as this process removes 97% of surface-produced opal leaving only 3% buried in the sediment record. There has been only one published laboratory study addressing Si isotope fractionation during opal dissolution, based on mixed-assemblage plankton trawl and sediment trap samples from the Southern Ocean (Demarest et al., 2009). The dissolution of this material under controlled conditions preferentially released the lighter isotopes of Si with a fractionation factor of -0.55 ‰. This would suggest that the progressive dissolution of sinking opal would result in a trend towards increasing $\delta^{30}Si$ within opal with depth. The limited data on the isotopic composition of suspended opal with depth in the water column (e.g. Fripiat et al., 2012), and the limited core top studies of biogenic opal (Egan et al., 2012; Wetzel et al., in review), show no indication of this trend. One hypothesis to explain this apparent discrepancy is that the dissolution of opal is not congruent among frustules with the majority of frustules found at depth or buried in sediments being relatively well preserved (note that <30% opal loss results in a non-detectable change in $\delta^{30}Si$, Demarest et al., 2009) with the remainder being nearly completely dissolved. Nelson et al (2002) found that in the Southern Ocean the opal that survives dissolution in the upper 1,000 m is nearly entirely delivered to the sea floor, consistent with the lack of changes in opal $\delta^{30}Si$ over this depth range in the Southern Ocean (Fripiat et al., 2012).

311 A dichotomy between frustules that completely dissolve and those that are well
312 preserved would largely eliminate the effect of dissolution in the water column from the
313 sediment record. However, other factors may be involved. Preliminary data on fractionation
314 of frustules recovered from sediments show little sign of fractionation during dissolution in
315 seawater (Beucher & Brzezinski, unpublished) suggesting the possibility of fundamental
316 differences in the effect of dissolution on fresh (Demarest et al, 2009) and preserved opal.
317 Other sedimentary processes such as precipitation of Si on diatom frustules (Ren et al., 2013)
318 have yet to be explored, along with the possibility of isotopic exchange with the high
319 concentrations of silicic acid in pore waters. It is clear that the question of the impact of
320 dissolution and abiotic precipitation/ isotope exchange on $\delta^{30}Si$ signatures must be addressed
321 with further studies of monospecific diatom cultures and different types of biogenic silica
322 (diatoms, sponges, radiolarians etc.) from different sources (fresh, preserved).

323 **5. Southern Ocean Influence on the Modern $\delta^{30}Si(OH)_4$ distribution**

324 Dynamics in the Southern Ocean are a major control on the distribution of $Si(OH)_4$,
325 and its isotope composition, on a global scale. South of the SACCF (Antarctic Divergence)
326 upwelled waters flow poleward and subduct with little biological removal of $Si(OH)_4$
327 resulting in the high dissolved Si concentrations of Circumpolar Deep Water (CDW) and
328 Antarctic Bottom Water (AABW) (e.g. Marinov et al., 2006). North of the Divergence Ekman
329 transport is equatorward and biological productivity is strong. Diatoms remove a high
330 fraction of the dissolved Si from surface waters, then sink with a portion of frustules
331 dissolving into the southward propagating deeper waters, returning to the Divergence as
332 dissolved $Si(OH)_4$. This recycling loop traps $Si(OH)_4$ in the Southern ocean water column.
333 Frustules that escape dissolution accumulate on the sea floor forming the Southern Ocean
334 opal belt, which – in the modern ocean – is the largest single locus of opal accumulation in
335 the sea and is located within the Antarctic sector of the Southern Ocean to the south of the

Polar Front.

Antarctic Intermediate Water (AAIW) and Sub-Antarctic Mode Water (SAMW) form by a combination of deep winter convection between the Polar Front and the Subantarctic Front (Bostock et al., 2013) and wind-driven mixing (Holte et al., 2012), forming the northward flowing shallow limb of the Meridional Ocean Circulation (MOC). AAIW and SAMW (collectively referred to as Southern Ocean Intermediate Waters, SOIW, after Pena et al., 2013) contain at least 10-15 µM silicic acid, but are depleted in $Si(OH)_4$ relative to other macronutrients (nitrate and phosphate), and it is these relatively low-silicon Mode Waters that feed into the thermocline in the lower latitudes. This can be traced by the parameter Si*, where $Si^* = [Si(OH)_4] - [NO_3^-]$. SOIW have negative Si* values, which can be seen far into the North Atlantic, Indian and Pacific Oceans (Sarmiento et al., 2004).

There has been recent attention paid to the role of MOC in oceanic silicon isotope distribution (de Souza et al., 2012a; de Souza et al., 2012b). In the high latitudes, in particular the Southern Ocean, uptake of the lighter isotopes of Si by diatoms imparts a heavy isotope signature (up to +2‰) in surface waters during the growth season, which is thought to be preserved in the winter mixed layer. The heavy isotope signature is transferred to the global thermocline via Mode Waters ($\delta^{30}Si(OH)_4 \sim +1.8‰$), and mixed into North Atlantic Deep Water (NADW, $\delta^{30}Si(OH)_4 \sim +1.6‰$) (Cardinal et al., 2005; Cardinal et al., 2007; de Souza et al., 2012b; Hendry et al., 2010). This is in contrast to deep waters in the Southern Ocean and Pacific, which have lighter $\delta^{30}Si(OH)_4$ signatures ($\delta^{30}Si(OH)_4 \sim +1.2‰$) as a result of opal remineralisation and the influence of the "production-free" signature of CDW and AABW (Beucher et al., 2008; De La Rocha et al., 2000; de Souza et al., 2012a).

5.1. Modelling global Si isotope distributions

Modelling of the global marine silicon isotope distribution requires special consideration of

360 deep remineralisation of opal compared to organic matter, and the important role played by
361 the Southern Ocean and, in particular, Mode Waters, which are poorly represented in many
362 climate models. The absolute isotope values obtained in simulations are also sensitive to the
363 δ^{30}Si of the Si entering the oceans, although the relative differences between ocean basins and
364 water masses are robust against the isotopic value of the assumed source. Rivers are the main
365 source of Si to the ocean (Tréguer et al. 1995) and have an average δ^{30}Si of +0.8‰ (De La
366 Rocha et al., 2000; Georg et al. 2006). The δ^{30}Si of river waters is mainly controlled by
367 weathering (Ziegler et al., 2005) and could vary under large climatic or tectonic changes on
368 time scales of 100,000 years or longer (De La Rocha and Bickle, 2005). Hydrothermal waters
369 are another source of Si to the sea (~10% the magnitude of the river source). Few $\delta^{30}Si(OH)_4$
370 data from hydrothermal fluids are available; two samples collected from vents on the East
371 Pacific Rise show negative values of -0.2 and -0.4‰ close to the average value for igneous
372 rock -0.3‰ (De La Rocha et al., 2000).

373 Wischmeyer et al. (2003) published the first simulation of the global distribution of
374 silicon isotopes in the world ocean using the Hamburg Model of the Ocean Carbon Cycle, V4.
375 This simulation relied on the assumptions that 1) fractionation during silica production is
376 constant with $\varepsilon_{DSi\text{-}BSi}$ = -1.1‰, 2) river inputs balance permanent Si burial in sediments and 3)
377 the dissolution of diatom frustules does not affect their isotopic composition (the study was
378 conducted prior to the discovery of fractionation during opal dissolution). Model output
379 showed the $\delta^{30}Si(OH)_4$ distribution in the surface waters to be inversely related to the
380 $Si(OH)_4$ concentrations in accordance with the expectation from Rayleigh fractionation of
381 increasing $\delta^{30}Si(OH)_4$ with greater $Si(OH)_4$ consumption. Plotting the two variables against
382 each other revealed that their relationship was not a simple Rayleigh distillation curve as the
383 isotopic composition of dissolved silicon not only traces its biological consumption, but also

384 the mixing of water masses with different $\delta^{30}Si(OH)_4$ signatures (Wischmeyer et al., 2003). A
385 puzzling result of the Wischmeyer et al. (2003) model was its failure to reproduce the
386 observed decrease in $\delta^{30}Si(OH)_4$ between the deep Atlantic and Pacific basins (De La Rocha
387 et al 2000), possibly due to an excess of nutrient drawdown in the Southern Ocean due to the
388 lack of iron limitation (Reynolds, 2009).

389 Multi-box models have been more successful in simulating silicon isotope
390 distributions (De La Rocha and Bickle, 2005; de Souza et al., 2012b; Reynolds, 2009), and
391 new generation GCMs are showing themselves to be promising with respect to reconstructing
392 the Si cycle. Reynolds (2009) used a seven box model (Toggweiler, 1999) and the ten-box
393 PANDORA box model (Broecker and Peng, 1987) to examine global marine silicon isotope
394 distributions. The results of the seven box model are presented here (Figure 4) although the
395 results from the PANDORA model are similar. Incomplete $Si(OH)_4$ use in the surface waters
396 of the Southern Ocean is a major driver of the model results. The dissolution of diatom
397 frustules formed under incomplete $Si(OH)_4$ consumption impart similarly light $\delta^{30}Si(OH)_4$
398 values to CDW/AABW. The northward flow of Southern Ocean water masses strongly
399 influences the isotopic composition of bottom waters in the Atlantic and Pacific basins.
400 Outside the Southern Ocean the isotopic signature of NADW in the model is largely set by
401 the strong ventilation in the north Atlantic.

402 *5.1.1. Agreement and discrepancies between simulations and measurements*

403 Comparison of the model results of Reynolds (2009) with the few measurements
404 available from the deep Atlantic and Southern Oceans shows both agreement and significant
405 anomalies between model predictions and data. The model predicts the observed relatively
406 heavy $\delta^{30}Si(OH)_4$ values in NADW and lighter values in CDW (Figure 5). The mechanisms
407 in the model leading to this gradient are the strong biological consumption of $Si(OH)_4$ in the

surface waters feeding into the well ventilated NADW combined with the effects of incomplete Si consumption in Southern Ocean surface waters mentioned above. The model was not constructed in a way to predict $\delta^{30}Si(OH)_4$ values of the deep waters of the Pacific (Figure 4, 5), but the PANDORA version of the model predicts a decrease in $\delta^{30}Si(OH)_4$ with increasing $[Si(OH)_4]$ along the MOC (Reynolds 2009).

Beucher et al. (2008)'s examination of the global deep water $\delta^{30}Si(OH)_4$ data set indicates that key mechanisms are operating in the Pacific that are not captured in current models. When data from waters >2,000 m in the Southern and Pacific Oceans are plotted as a function of $1/[Si(OH)_4]$ most data fall along a single straight line suggesting that a simple mixing model can explain most results (Figure 5). The high concentration end member is the Northeast Pacific Silicic Acid Plume that originates in the Cascadia Basin (Johnson et al., 2006) that has $[Si(OH)_4]$ >150 µM corresponding to a $1/[Si(OH)_4]$ value of ~0.005 in Figure 5. The other end member lies in the Southern Ocean. In contrast, the data from the North Pacific and the Northwest Pacific fall on a trajectory of decreasing $\delta^{30}Si(OH)_4$ with increasing $[Si(OH)_4]$ from the Atlantic to the Southern Ocean and Pacific as predicted by models (Reynolds 2009).

A hypothesis that explains the anomalous isotope patterns in the Pacific is that the Northeast Pacific $Si(OH)_4$ Plume (Johnson et al. 2006) exerts a major influence on Si isotopes in this region. The flux of $Si(OH)_4$ from the sediments beneath the Plume is large (1.5 Tmol Si a^{-1}) equivalent to a third of that supplied to the global ocean by rivers (Johnson et al. 2006). Its influence extends to the west and to the south, but apparently not as far west as the stations in the North Pacific (23°N, 158°W, De La Rocha 2000) and NW Pacific (24.3°N, 170.3°W) presented in Figures 5. This feature has not been incorporated into models of Si isotope distributions. Note that the $\delta^{30}Si(OH)_4$ of the waters in the Plume, +1.4‰, is much more

positive than hydrothermal sources (~ -0.3‰, De La Rocha et al., 2000) suggesting a biogenic source. The $\delta^{30}Si(OH)_4$ of the Plume is similar to that in the North Atlantic (Figure 5) so that it's influence essentially eliminates contrasts in $\delta^{30}Si(OH)_4$ between the deep Atlantic and deep Northeast Pacific.

The main point to be taken from this analysis is that the spatial resolution of the present $\delta^{30}Si(OH)_4$ data set is inadequate to evaluate mechanisms leading to even the first-order distribution of isotopes of Si in the global ocean although strong anomalies point to possible explanations. The level of variability in $\delta^{30}Si(OH)_4$ within Pacific deep waters far exceeds that predicted by current models and trends between Si isotopes and Si concentration are opposite of model predictions, possibly due the Northeast Pacific Silicic Acid Plume, but other unanticipated mechanisms may be involved. New data from the International GEOTRACES program that is producing sections of $\delta^{30}Si(OH)_4$ distributions along several major ocean sections should help resolve these issues.

6. Paleoceanographic applications and multi-proxy approaches

In addition to the whole-ocean concentration, biogenic opal production is controlled by the distribution of $Si(OH)_4$ in the global ocean. Since their evolution, diatoms have dominated the marine silicon cycle and opal formation, such that they have effectively stripped $Si(OH)_4$ out of surface waters (Falkowski et al., 2004), resulting in pervasive Si limitation of silica production (or co-limitation with other nutrients e.g. iron) in low latitude regions (e.g. Brzezinski et al., 2008; Brzezinski and Nelson, 1996). Net diatom production relies on upwelled sources of dissolved silicon; changes in ocean circulation and upwelling are therefore key to controlling opal production and carbon drawdown by diatoms.

Particular hypotheses that have received attention over the last decade are the Silicic Acid Leakage Hypothesis (SALH; Brzezinski et al., 2002; Matsumoto et al., 2002) and the

456 related silica hypothesis (Harrison, 2000; Nozaki and Yamamoto, 2001). The silica
457 hypothesis states that diatom productivity was promoted during glacials as a result of an
458 increase in Si supplied from dust, contributing to the drawdown of CO_2 (Harrison, 2000). In
459 contrast, the SALH posits that, during Pleistocene glacials, the addition of iron via enhanced
460 dust deposition in the Southern Ocean results in a change in diatom physiology, such that
461 diatoms take up macronutrients at a lower Si:N ratio. This arises from the combination of
462 decreased cellular N content in most, if not all diatoms, and the thickening or thinning of the
463 siliceous frustules in response to low Fe (Hutchins & Bruland 1998, Takeda, 1998, Marchetti
464 & Harrison 2007). Even in cases where diatoms thin their frustules in response to low Fe
465 (Marchetti & Harisson 2007) the reduction in cellular N is even greater such that increased
466 Si:N is a universal response. The addition of Fe to modern day Southern Ocean waters shifts
467 Si:N uptake ratio from a value of 4-8 under ambient conditions to a value of 2 (Frank et al.
468 2000). Given the $[Si(OH)_4[:[NO_3^-]$ ratio of ~2.3 in upwelling waters at the Antarctic
469 Divergence, release from Fe stress during glacial times would cause approximately half of the
470 upwelled silicic acid to remain in surface waters upon nitrate depletion (Brzezinski et al,
471 2002). The net result is that the water which subducts to form the all-important SOIW that
472 ultimately feed the lower latitude thermocline, would have both higher $[Si(OH)_4]$ and a higher
473 Si:N ratio. Ventilation of the relatively Si-rich SOIW at low latitude would promote the
474 growth of diatoms relative to carbonate producers, altering the $C_{org}/CaCO_3$ rain ratio and
475 ocean alkalinity to lower atmospheric CO_2 (Matsumoto and Sarmiento, 2008; Rickaby et al.,
476 2007). Opal-based silicon isotope proxies are ideal tools for investigating the SALH, and to
477 investigate other past changes in the marine silicon cycle (Figure 6).

478 ***6.1. Silicic acid leakage from the Southern Ocean***

479 *6.1.1. Opal mass accumulation rates and $^{231}Pa/^{230}Th$*

480 For the SALH to be accepted, there has to be evidence for a change in Si utilization in the

481 Southern Ocean, which would have provided the excess $Si(OH)_4$ to escape to lower latitudes.
482 Records of Southern Ocean opal mass accumulation rates (MAR) since the Last Glacial
483 Maximum (LGM) provide a consensus view that the main belt of opal deposition around
484 Antarctica shifted northwards compared to today, into the subantarctic zone (reviewed by
485 Bradtmiller et al., 2009). These records also imply that there was no net increase in opal
486 production that could have contributed to a drawdown of atmospheric pCO_2 in either the
487 Atlantic or Indian Sectors of the Southern Ocean (Frank et al., 2000; Kumar, 1995).
488 However, there was a decrease during the LGM of total mass flux in the Pacific Sector, which
489 is the main candidate for potential leakage of $Si(OH)_4$ to the lower latitudes (Bradtmiller et
490 al., 2009; Chase et al., 2003a).
491 *6.1.2. Opal isotope proxies*
492 *Si isotope records*
493 Glacial-interglacial changes in Si utilization by diatoms south of the modern Antarctic
494 Polar Front was the first paleoclimate question to be addressed using the diatom opal $\delta^{30}Si$
495 proxy (De La Rocha et al., 1998). These first diatom $\delta^{30}Si$ records showed that there was a
496 lower Si utilization south of the Antarctic Polar Front at the LGM compared to today, and this
497 finding has also been mirrored in sediment cores from the subantarctic (Beucher et al., 2007),
498 supporting the SALH. A reduction in utilization is consistent with a decline in Si uptake by
499 diatoms, relative to other nutrients, as a result of the alleviation of Fe stress. However,
500 changes in dissolution and water column recycling processes, as a result of the alteration of
501 the recirculation that produces the modern silicon trap, could also be responsible for the
502 observed shifts in diatom $\delta^{30}Si$.
503 *Si-N isotope records*
504 The preferential and variable uptake of $Si(OH)_4$ over NO_3 in the low-iron waters of
505 the Southern Ocean seawater results in a decoupling of the dynamics of these two

506 macronutrients and the preferential depletion of $Si(OH)_4$ over NO_3 in the modern Southern
507 Ocean (Pondaven et al., 2000). The relative utilization of the two nutrients has been
508 constrained over time using combined Si and N isotope records from diatom opal and opal-
509 bound organic matter respectively. One of the principal aims to date has been to investigate
510 changes in Si:N uptake rates in the Southern Ocean over glacial-interglacial timescales as a
511 test of the SALH (Beucher et al., 2007; Crosta et al., 2007; Horn et al., 2011; Robinson et al.,
512 2005b). Although there are analytical challenges surrounding the robust application of
513 diatom-bound N isotopes (Robinson et al., 2004), these studies generally agree that there was
514 relatively higher utilization of N in surface waters compared to $Si(OH)_4$ during the Last
515 Glacial Maximum, suggesting a relatively high Si:N ratio in Mode Waters, and supporting the
516 SALH (e.g. Horn et al,. 2011). More recent studies are beginning to delve into $Si(OH)_4$
517 leakage deeper in time, such as an investigation of the role of southern sourced water in
518 driving the highly productive Matuyama Diatom Maximum in the Benguela Upwelling
519 System (Ocean Drilling Program Site 1082, 21.1 ºS, 11.8 ºE, 1279m water depth) from 2-3
520 Ma (Etourneau et al., 2012). The heaviest diatom $\delta^{30}Si$ signal corresponded with the highest
521 opal accumulation rate, and the lightest diatom-bound $\delta^{15}N$, which could be explained by the
522 growth of mat-forming diatoms due to an increased $Si(OH)_4$ supply from southern sourced
523 water, but weak upwelling. The mat-forming diatoms efficiently utilised a large proportion of
524 the available Si, resulting in Si-limitation of surface waters and relatively low N utilization
525 (Etourneau et al., 2012).

526 *Paired diatom-sponge Si isotopes*

527 In an analogous fashion to paired benthic-planktonic foraminifera carbon isotopes,
528 paired sponge-diatom silicon isotope records can be used to quantify the marine silicon cycle
529 of the whole water column: the supply of dissolved $Si(OH)_4$ from deep waters, and the
530 utilization of silicon in surface waters by diatoms in the Southern Ocean. To date, the multi-

proxy approach has been used to investigate the SALH since the Last Glacial Maximum (Hendry et al., 2010; Hendry et al., 2012; Horn et al., 2011). These studies have been able to constrain deep water $Si(OH)_4$ concentrations (Hendry et al., 2010) and the upwelling rate of $Si(OH)_4$ (Horn et al,. 2011). The records show a dramatic increase in upwelling supply, confirmed an increase in the utilization of Si (Horn et al,. 2011), and a slight transient decrease in the concentration of $Si(OH)_4$ in deep waters across the last glacial termination (Hendry et al., 2010).

Paired Si-Ge records

One important caveat that needs to be considered when reconstructing [$Si(OH)_4$] from sponge spicule $\delta^{30}Si$ using equation 5 is that the isotopic composition of the $Si(OH)_4$ is required to calculate $\Delta\delta^{30}Si$. Thus the estimated $Si(OH)_4$ concentration is a function of the measured spicule $\delta^{30}Si$ and for paleo - reconstructions, the assumed deep water $\delta^{30}Si(OH)_4$. As discussed above deep water $\delta^{30}Si(OH)_4$ is tied to water mass distributions within the MOC in the modern. Deviations from the modern in the past will depend both on i) the secular shift in whole ocean $\delta^{30}Si$ through time, on timescales greater than the residence time of Si in the global oceans (~10 ka, Georg et al., 2009; Tréguer and De la Rocha, 2013), for example due to changes in subglacial weathering processes and meltwater inputs to the ocean (Opfergelt et al., 2013); and ii) on changes in the distribution of silicon isotopes in the oceans resulting from ocean circulation changes, on timescales of thousands of years or more.

Previous studies have taken these changes into account through simple modelling efforts (e.g. Hendry et al., 2012; Griffiths et al., 2013) or by pairing with diatom $\delta^{30}Si$ (Egan et al, 2012). However, an alternative approach is to use, in addition to spicule $\delta^{30}Si$, sponge and diatom Ge/Si ratios. Spicule Ge/Si will record not only secular changes in seawater Ge/Si, which can be corrected for using diatom Ge/Si (thought to be a recorder of secular

555 changes in whole ocean Ge/Si, although there needs to be a more thorough assessment of
556 vital effects (Froelich et al., 1992), but also a component of $Si(OH)_4$ concentration. In other
557 words, spicule $\delta^{30}Si$ and Ge/Si provide complementary access to past ocean $Si(OH)_4$
558 concentrations. This approach has been used to investigate the SALH: Ge/Si and Si isotope
559 proxies in sediment cores from the Atlantic and Pacific Sectors (~41ºS, ~10ºE, 4600m water
560 depth, and ~53ºS, ~120ºW, 2700m water depth) of the Southern Ocean show that there was a
561 build-up of nutrients during glacial periods in the Pacific Sector only, consistent with opal
562 accumulation records (Bradtmiller et al., 2009; Chase et al., 2003a; Ellwood et al., 2010).

563 ***6.2. Impact of silica leakage on the low latitudes***

564 *6.2.1. Opal accumulation rates*

565 Records of opal mean accumulation rate (MAR), ^{230}Th-normalised opal MAR, and
566 downcore $^{231}Pa/^{230}Th$ do not reveal a clear picture of changes in low latitude diatom
567 productivity over glacial-interglacial and millennial timescales in response to $Si(OH)_4$
568 leakage, pointing towards multiple controls in Si supply and uptake. In the Central and
569 Eastern Equatorial Pacific, and the Peru upwelling zone, ^{230}Th-normalised opal fluxes are
570 higher at Marine Isotope Stage (MIS) 3 (~30-60 ka) than during MIS2 (~20-30 ka), with
571 either similar or lower opal fluxes during the Last Glacial Maximum compared to the
572 Holocene, which is inconsistent with the SALH (Bradtmiller et al., 2006; Kienast et al., 2006;
573 Richaud et al., 2007). However, records going back further into the Pleistocene show higher
574 ^{230}Th-normalised opal fluxes at the glacial terminations than at full glacial conditions or
575 during interglacials, but these peaks are not observed for all terminations, and there are peaks
576 in opal flux not associated with terminations (Bradtmiller et al., 2006; Dubois et al., 2010;
577 Hayes et al., 2011). In contrast, the Eastern Tropical North Pacific (ETNP) shows higher opal
578 MAR at the glacials compared to the interglacials (Arellano-Torres et al., 2011). In the
579 Western Pacific, large diatom mats in the Phillipines Sea, comprising *Ethmodiscus rex*, have

been carbon dated to MIS2 (Zhai et al., 2009). However, $^{231}Pa/^{230}Th$ and ^{230}Th-normalised opal fluxes from another core in the Western Equatorial Pacific indicates lower productivity in glacial periods (Pichat et al., 2004).

Similar inconsistencies occur in the Atlantic. In the Equatorial Atlantic, the sediment cores that have been analyzed to date show higher opal accumulation and corresponding $^{231}Pa/^{230}Th$ during the last glacial, with peaks occurring at the deglaciation, although these cores do not have sufficient sedimentation rates to resolve fully Heinrich Stadials, the abrupt climate events of the late glacial and deglacial (Bradtmiller et al., 2007). Other sites in the Eastern North Atlantic show clearer abrupt increases in opal export during the deglacial, which correspond with oceanic and/or atmospheric reorganisation during the Heinrich Stadials (Meckler et al., 2013; Romero et al., 2008).

In addition to inherent preservation bias, there are a number of reasons why the low latitude opal accumulation rate records need to be treated carefully in the context of the SALH. Firstly, the opal MAR records reveal complex temporal and spatial patterns, reflecting a number of regional and local controls on productivity. Secondly, tropical opal burial reconstructions cannot distinguish between the silica hypothesis of Harrison (2000) and the SALH *senso stricto* (Brzezinski et al., 2002) i.e. opal records cannot provide a mechanistic interpretation for productivity changes. Thirdly, $Si(OH)_4$ leakage may not manifest in an increase in opal accumulation rate, *per se*, but an increase in the productivity of opal-producers relative to carbonate producers, and still produce a shift in ocean alkalinity and pCO_2 drawdown (Matsumoto & Sarmiento, 2008). In other words, the lack of a coherent change in low latitude opal accumulation rates is not sufficient to reject the SALH. Instead, a multi-proxy approach allows the various interacting controls on productivity to be deconvolved, and specific hypotheses regarding the SALH to be tested.

6.2.2. Multi-proxy isotope records of low latitude changes in water mass and ecology

Sponge spicule silicon isotopes

An important concept that follows from the SALH is that intermediate waters subducting away from the Southern Ocean must have increased in $Si(OH)_4$ during the glacial. Sponge spicule $\delta^{30}Si$ records of benthic $Si(OH)_4$ concentrations provides one of the most direct methods for testing this assertion. Spicule isotopic records from core site GeoB2107-3 (27°S, 46°W, 1050 m water depth), which is bathed in modern AAIW, show that the $Si(OH)_4$ concentrations were not significantly different at the LGM compared to today. However, the records show pulses of heavy $\delta^{30}Si$ – indicative of high $Si(OH)_4$ concentrations – during the abrupt events of the late glacial and deglacial, Heinrich Stadials (HS) One and Two, and the Younger Dryas (Hendry et al., 2012). In other words, leakage of high Si waters from the Southern Ocean to lower latitudes occurs, but during abrupt climate change events rather than on glacial-interglacial timescales.

Paired Si-Nd isotopes

Due to biogeographical variations and ocean circulation, Southern Ocean deep waters are characteristically $Si(OH)_4$-rich, and changes in their $Si(OH)_4$ content can be traced by the $\delta^{30}Si$ of benthic sponge spicules (Hendry et al., 2010). The Nd isotope composition (εNd) of bottom water, recorded in fish teeth, sediments, and Fe-Mn coatings of planktonic foraminifera in some oceanographic settings (e.g. Pahnke et al., 2008; Piotrowski et al., 2008; Roberts et al., 2010), provides an additional method of "labelling" southern sourced waters, due to a distinctive radiogenic signature from mixing with Pacific waters (Albarede et al., 1997). However, one key problem with the εNd proxy is that the Nd southern and northern end members could change over relevant timescales (Pahnke et al., 2008). The part of the water column that is represented by planktonic foraminiferal coatings is also apparently variable (Pena et al., 2013; Roberts et al., 2010). A combination of these benthic $\delta^{30}Si$ and

εNd can, however, provide a more robust means of tracing southern sourced water.

To date, this has been used to investigate the SALH across MIS4 (~60-70 ka) in the tropical Atlantic (Griffiths et al., 2013), and more localised processes in the Peruvian upwelling zone of the South Pacific (Ehlert et al., 2013). Of relevance to the SALH, Griffiths et al. (2013) found that both "tracers" indicated an increase in the presence of southern component water in a sediment core off the coast of Brazil (core site MD99-2198, 12.09ºN; 61.23ºW; 1330m water depth) across the MIS 5/4 boundary, consistent with a modest leakage of relatively Si-enriched water from the Southern Ocean at this time via SOIW. However, further work is required to understand the relationship between these two proxies, given the slight differences in the timing and nature of the changes recorded in core MD99-2198.

Si-N isotopes

Diatom Si and diatom-bound N isotopes from a core in the Eastern Equatorial Pacific support a reduction in Si uptake relative to other nutrients due to the alleviation of Fe stress – and limitation by Si and N - during the glacial. The authors argue for a fundamental change in nutrient limitation in the region, with a likely glacial switch to phosphorus limitation away from Si-Fe co-limitation (Pichevin et al., 2009).

7. Silicic Acid Leakage form the Southern Ocean – New Insights and Changing Perspectives

The SALH has been tested repeatedly over the past few years. One of the key issues, and the main defining difference between the silica hypothesis (Harrison , 2000) and the SALH *senso stricto* (Brzezinski et al., 2002), is the extent to which SOIW distributions have changed over glacial-interglacial and millennial timescales. Other geochemical archives have been used to investigate changes in intermediate water formation and distribution, including stable carbon isotopes (Spero and Lea, 2002; Bostock et al., 2004; Pahnke & Zahn, 2005; Bostock et al., 2010), diatom-bound carbon isotopes (Xiong et al., 2013), radiocarbon (Burke

654 and Robinson, 2011; Keigwin, 2004; Mangini et al., 2010; Robinson et al., 2005a; Thornalley
655 et al., 2011), εNd (Pahnke et al., 2008; Pena et al., 2013; Xie et al., 2012), and biomarkers
656 (Calvo et al., 2004; Calvo et al., 2011; dos Santos et al., 2012; Higginson and Altabet, 2004).
657 Some coherent pictures have begun to arise of expanded AAIW during glacials, especially in
658 the Pacific (Bostock et al., 2004, 2010), with intense deep mixing with CDW and Glacial
659 Antarctic Bottom Water (GAABW), expanded oligotrophic surface waters in the Subantarctic
660 and so a strong subsurface nutrient gradient (Bostock et al., 2004, 2010). Furthermore, carbon
661 isotopes suggest widespread pulses of well-ventilated SOIW formation during the Heinrich
662 Stadials and Younger Dryas (Pahnke & Zahn, 2005).
663 Other lines of evidence point towards expanded SOIW during abrupt climate events of
664 the deglacial e.g. Nd isotope record from the Tobago Basin and East Equatorial Pacific
665 (Pahnke et al,. 2008; Pena et al,. 2013). Another εNd record from the Florida Straits points
666 towards reduced SOIW presence in the North Atlantic during Heinrich Stadial One and the
667 Younger Dryas (Xie et al., 2012). However, this study assumed almost pure AAIW filled the
668 study site basin, an assumption that is not supported by modern hydrographic data (Pena et
669 al., 2013). These disagreements highlight the complex nature of reconstructing oceanic
670 circulation, and the problems with geochemical proxies, for example in terms of signal
671 redistribution (Gutjahr et al., 2008) and changing water mass end-members (Pahnke et al.,
672 2008).
673 The opal-based evidence from the Southern Ocean discussed above, combining opal
674 δ^{30}Si records with other palaeoproxies, indicates that there were major ecological changes in
675 the Southern Ocean over glacial-interglacial timescales, which would have led to a change in
676 the composition of SOIW. The Si:N ratio would increase during glacials either due to a
677 change in i) utilization of Si relative to N as a result of Fe fertilization (Brzezinski et al.,
678 2002), or ii) the location of the opal belt such that dissolution and regeneration of opal occurs

679 in the region of SOIW subduction (Bradtmiller et al., 2007). However, proxy evidence from
680 low latitudes suggests that, on glacial-interglacial timescales, the impact on lower latitude
681 ecology, and climate, was minimal. A reduction in the rate of SOIW supply, or indeed a
682 change in the depths to which the subducted waters penetrated, over glacial-interglacial
683 timescales may have limited the extent to which the southern sourced preformed nutrients
684 could upwell in the low latitudes (Crosta et al., 2007). Rather, it was changes on abrupt
685 (millennial) timescales in ocean circulation and wind-driven upwelling (Anderson et al.,
686 2009; Moreno et al., 2002) during glacial terminations that enhanced the supply of – most
687 likely – southern sourced Si-rich water that drove the major ecological changes observed in
688 lower latitude sedimentary cores (Pahnke et al., 2008; Hendry et al., 2012; Calvo et al., 2011;
689 Bradtmiller et al., 2008). The most-cited sources for these southern-component waters are
690 SOIW (e.g. Pahnke et al., 2008; Calvo et al., 2011; Pena et al., 2012; Hendry et al., 2012),
691 which are known to feed the lower thermocline with nutrients in the low latitudes (Sarmiento
692 et al., 2004). However, it has also been speculated that the $Si(OH)_4$ feeding the low latitude
693 peaks in opal production seen in the Equatorial and North Atlantic originated from upwelling
694 deep southern component water through a large-scale change in ocean circulation (Meckler et
695 al., 2013). However, the similarity of the deglacial opal peaks in the low-latitude Atlantic and
696 Pacific Oceans (Bradtmiller et al., 2006, 2007) would require a process that could operate in
697 both basins despite the different deep-water mass configurations, and so could be used to
698 argue against a deep southern component water mechanism.
699 Could changing nutrient dynamics in the Southern Ocean alter southern-sourced
700 Mode Waters to cause major changes in nutrient distribution during abrupt climate change?
701 Whilst a speculative twist on the SALH, such events may be the logical outcome of the shifts
702 in Southern Ocean circulation and nutrient supply during glacial terminations. Glacial
703 periods are characterized by the northward shift in the westerly winds in the Antarctic coupled

with strong stratification south of the Polar Front due to buoyancy-forcing and reduced wind-stress (Marshall & Speer, 2012). Diatom productivity and the opal belt also shifted northward supported mainly by upwelling within the Subantarctic (Beucher et al., 2007, Bostock et al., 2004). Upwelling and mixing to the north of the Polar Front in the Subantarctic would not be as efficient in tapping high-nutrient deeper waters compared to the circulation associated with the Antarctic Divergence, diminishing nutrient supply during glacials. The northward shift in the opal belt may have been coupled with a reduction in residual silicic acid concentrations as a result of a lower supply of Si to the Subantarctic surface waters and significant diatom production. Combined with high atmospheric Fe supply this would result in SOIW with high Si:N ratio, but diminished Si concentrations. Hence, SOIW mixing with low-latitude thermocline waters did not promote significant diatom growth, especially in regions where wind-driven upwelling was also weakened during glacial times (e.g. Moreno et al., 2002). However, during HS1, sustained Fe supply to the Southern Ocean, continued mixing in the Subantarctic (e.g. Bostock et al., 2004), together with a breakdown of stratification and increased upwelling in the Antarctic (e.g. Anderson et al., 2009; Burke & Robinson, 2011) would re-establish the Antarctic Divergence and - once again – lead to the efficient tapping of deeper waters. Such an increase in upwelling would result in an increase in both Si and oceanic Fe supply to surface waters (Ayers & Strutton, 2013), despite reducing atmospheric Fe input (Lambert et al., 2008). Strong wind-driven mixing would result in deep winter convection (Holte et al., 2012) and formation of SOIW with high Si concentrations and high Si:N. At the same time, enhanced wind-driven upwelling in the lower latitudes increased the supply of these waters to the thermocline and so supported enhanced diatom growth. Whilst the atmospheric Fe supply to the surface of the Southern Ocean had declined by the Younger Dryas (Lambert et al., 2008), and the Southern Ocean Si trap was re-established, low-latitude diatom pulses still occurred in places of enhanced wind-driven upwelling as a response to

729 enhanced mixing of oceanic Fe in the Subantarctic and changes in the vertical structure of
730 SOIW (Hendry et al., 2012).

731 Key to this scenario is the change in the efficiency with which Southern Ocean
732 circulation brings abyssal waters with high nutrients to the surface where opal formation
733 occurs. During the glacials, that efficiency is low due to increased stratification and reduced
734 mixing in Antarctic waters coupled with the northwards shift in the opal belt from the
735 Antarctic Divergence to the Subantarctic, where entrainment of high-nutrient abyssal water is
736 less pronounced. A southwards shift in the opal belt and enhanced upwelling and mixing in
737 the Antarctic Divergence during Heinrich Stadials would increase the efficiency of oceanic
738 nutrient supply from deep waters, and both the Si content and Si:N ratio of mode waters
739 (Ayers & Strutton, 2013). Together these factors form the basis of a **"Silicic Acid**
740 **Ventilation Hypothesis" (SAVH) (**Figure 7) where the change in oceanic and atmospheric
741 circulation that occurred during the Heinrich Stadials would lead both to the ventilation of
742 waters near the Antarctic Divergence, resulting in Si-enriched SOIW, and the low-latitudes,
743 leading to the supply of these high Si waters to the surface and triggering the widespread and
744 abrupt ecological changes that are observed. Further investigation into intermediate depth
745 water composition, using high-resolution records of diatom and spicule $\delta^{30}Si$, in addition to
746 the other proxies discussed above, will be able to test the plausibility of such a mechanism.

747 The original SALH proposed that Si leakage during glacial times contributed to global
748 cooling by lowering atmospheric pCO_2 during glacial periods. The more recent evidence that
749 Si leakage from the Southern Ocean occurred predominately during deglaciations has
750 profound implications for the effect of this mechanism on climate. Si leakage during
751 deglaciations would drive low latitude flora towards diatoms when atmospheric pCO_2 levels
752 were rising. This suggests that the ecological effects that would favour a decline in
753 atmospheric pCO_2 was overwhelmed by other, possibly physical processes, such as the

increased evasion of CO_2 from the ocean due to increased upwelling at the Antarctic Divergence (Anderson et al 2009).

8.**Synthesis and Conclusions**

The Southern Ocean plays a key role in the climate system, through heat and nutrient transfer to the global oceans. The "biogeochemical divide" formed by the Antarctic Divergence, and the formation of Mode Waters, essentially sets the global levels of preformed nutrients and stored carbon (Marinov et al., 2008; Marinov et al., 2006; Sarmiento et al., 2004; Sigman et al., 2010). Understanding Mode Water nutrients, and how they have changed in the past, is essential for understanding past changes in both Southern Ocean and low latitude biological productivity. Diatoms dominate the phytoplankton communities in most regions of the Southern Ocean, and they impart distinctive $Si(OH)_4$ concentrations and isotope signatures on the subducting waters that form the Mode Waters. The established relationship between isotopes of Si and the MOC allows the proxy to be used as both a nutrient proxy and an indicator of water mass changes. Furthermore, biogenic opal provides an important archive of past ocean biological productivity and environmental conditions in the Southern Ocean and beyond. In particular, when used in conjunction with other sedimentary proxies, biogenic opal $\delta^{30}Si$ has shown itself to have great potential in deconvolving past signals of climatic, biogeochemical and ecological change.

Acknowledgements

KH is funded by the Royal Society, the Climate Change Consortium of Wales, the Natural Environment Research Council, and the Leverhulme Trust. MB is funded by the US National Science Foundation.

Figure 1:

Schematic of the transport of $Si(OH)_4$ in the ocean and the relationship with the MOC, after Marinov et al. (2008). The double-headed arrows show the major water masses, shaded according to $Si(OH)_4$ concentration. The dashed line shows the thermocline depth.

Figure 2:

Apparent fractionation factors estimated from a number of culture, water column and sediment core top studies. (Beucher et al., 2008; Cao et al., 2012; Cardinal et al., 2005; De La Rocha et al., 1997; De La Rocha et al., 2011; Egan et al., 2012; Ehlert et al., 2013; Fripiat et al., 2012; Fripiat et al., 2011; Milligan et al., 2004; Reynolds et al., 2006; Sutton et al., 2013; Varela et al., 2004).

Figure 3:

$\Delta\delta^{30}Si$ for all sponges from different ocean basins. The modern sponges (open symbols) were measured without Mg doping, with error bars showing 2SD (~±0.2 ‰ for $\delta^{30}Si$ and 0.4 ‰ for $\Delta\delta^{30}Si$). The core-top spicules (solid symbols) were measured with Mg doping, with error bars showing 2SD (~±0.1 ‰ for $\delta^{30}Si$). Unless specified, data are from Hendry & Robinson, 2012.

Figure 4:

Results using a seven box model simulating $Si(OH)_4$ concentrations and $\delta^{30}Si$ $(OH)_4$ distributions (italics in parentheses). Surface boxes from left to right correspond to the Antarctic, Subantarctic, Low Latitude surface waters and the Subarctic. Adapted from Reynolds (2009). Abbreviations taken from Reynolds (2009): AAIW = Antarctic Intermediate Water (essentially Mode Waters comprising Antarctic Intermediate Waters and Subantarctic Mode Water); CDW = Circumpolar Deep Water; NADW = North Atlantic Deep Water.

Figure 5:

$\delta^{30}Si$ versus $1/[Si(OH)_4]$ for waters below 2000 m (adapted from Beucher et al., 2008). EEP, Eastern equatorial Pacific; AZ, Antarctic Zone; SAZ, Subantarctic Zone; PFZ, Polar Frontal Zone; HOTS, Hawaiian Oceanic Time Series; BaTS, Bermuda Time Series. Linear regression of data from Southern Ocean and Eastern Pacific. Gray line drawn by eye. Model results from Reynolds (2009).

Figure 6:

Map showing location of studies specifically aimed at investigating the SALH. Drawn using Ocean Data View. (Arellano-Torres et al., 2011; Beucher et al., 2007; Bradtmiller et al., 2006, 2007, 2009; Calvo et al., 2004; Calvo et al., 2011; Chase et al., 2003a; Crosta et al., 2007; De La Rocha et al., 1998; dos Santos et al., 2012; Dubois et al., 2010; Ehlert et al., 2013; Ellwood et al., 2010; Frank et al., 2000; Hayes et al., 2011; Hendry et al., 2010; Hendry et al., in revision; Hendry et al., 2012; Higginson and Altabet, 2004; Horn et al., 2011; Kienast et al., 2006; Kumar, 1995; Meckler et al., 2013; Pena et al., 2013; Pichat et al., 2004; Pichevin et al., 2010; Pichevin et al., 2009; Richaud et al., 2007; Robinson et al., 2005b; Romero, 2010; Romero et al., 2011; Zhai et al., 2009)

Figure 7:

Cartoon illustrating the **"Silicic Acid Ventilation Hypothesis" (SAVH).** LCDW = Lower Circumpolar Deep Water; GNAIW = Glacial North Atlantic Intermediate Water; GAABW = Glacial Antarctic Bottom Water; SOIW = Southern Ocean Intermediate Water. The black triangle shows the location of the Southern Ocean opal belt.

During the LGM, Mode Waters formed with a high Si:N ratio, due to changes in utilization and dissolution processes resulting from Fe fertilization and a northwards movement of the opal belt (Bradtmiller et al., 2009). Buoyancy-driven stratification in the Southern Ocean and

824 weaker mixing in the Subantarctic , coupled with weaker upwelling in key regions (e.g.
825 Benguela Upwelling System, (Romero, 2010)) increases the ratio of Si:N in SOIW, but
826 reduces the concentration of Si, and so reduces the supply of Si to low-latitude thermocline
827 waters.
828 At Heinrich Stadial 1 (HS1, 16-18 ka), ice-rafting in the North Atlantic drives a collapse of
829 GNAIW (McManus et al., 2004), a southwards shift of the Atlantic Intertropical Convergence
830 Zone (ITCZ), a strengthening of the NE Trade Winds (Vink et al., 2001) and a southwards
831 shift in the Southern Ocean Westerlies (Anderson et al., 2009). These atmospheric changes
832 could have resulted in stronger upwelling in some regions of the North Atlantic and Pacific
833 Oceans (Koutavas and Sachs, 2008; McClymont et al., 2012). Enhanced wind-driven
834 upwelling, and greater mixing in the Subantarctic, together with a breakdown of buoyancy-
835 driven stratification in the Southern Ocean, would have led to high Si:N and high Si
836 concentration SOIW. A concurrent increase in ventilation in the Southern Ocean and the low-
837 latitudes would have led both to an export of these high Si:N and high [Si] waters and an
838 increase in their supply to thermocline and surface waters, promoting low-latitude diatom
839 production.

840 Albarede, F., Goldstein, S. L., Dautel, D., 1997, The neodymium isotopic composition of
841 manganese nodules from the Southern and Indian Oceans, the global oceanic
842 neodymium budget, and their bearing on deep ocean circulation. Geochimica et
843 Cosmochimica Acta 61 (6), 1277-1291.
844 Andersen, M. B., Vance, D., Archer, C., Anderson, R. F., Ellwood, M. J., Allen, C. S., 2011,
845 The Zn abundance and isotopic composition of diatom frustrules, a proxy for Zn
846 availability in ocean surface seawater. Earth and Planetary Science Letters301, 137-
847 145.
848 Anderson, R. F., Ali, S., Bradtmiller, L. I., Nielsen, S. H. H., Fleisher, M. Q., Anderson, B. E.,
849 Burckle, L. H., 2009, Wind-driven upwelling in the Southern Ocean and the deglacial
850 rise in atmospheric CO2. Science 323, 1443-1448.
851 Arellano-Torres, E., Pichevin, L. E., Ganeshram, R. S., 2011, High-resolution opal records
852 from the eastern tropical Pacific provide evidence for silicic acid leakage from HNLC
853 regions during glacial periods. Quaternary Science Reviews 30, (9-10), 1112-1121.
854 Ayers, J.M., Strutton, P.G., 2013, Nutrient variability in Subantarctic Mode Waters forced by
855 the Southern Annular Mode and ENSO. Geophysical Research Letters, 40, 3419–
856 3423,
857 Beucher, C. P., Brzezinski, M. A., Crosta, X., 2007, Silicic acid dynamics in the glacial sub-
858 Antarctic: Implications for the silicic acid leakage hypothesis. Global Biogeochemical
859 Cycles 21, doi:10.1029/2006GB002746.
860 Beucher, C. P., Brzezinski, M. A., Jones, J. L., 2008, Sources and biological fractionation of
861 silicon isotopes in the Eastern Equatorial Pacific. Geochimica et Cosmochimica Acta
862 72, 3063-3073.
863 Bostock, H.C., Opdyke, B.N., Gagan, M.K., Fitfield, L.K., 2004, Carbon isotope evidence for
864 changes in Antarctic Intermediate Water circulation and ocean ventilation in the
865 southwest Pacific during the last deglaciation. Paleoceanography 19,
866 doi:10.1029/2004PA001047.
867 Bostock, H.C., Opdyke, B.N. Williams, M.J.M., 2010, Characterising th intermediate depth
868 waters f the Pacific Ocean using $\delta^{13}C$ and other geohemical tracers: Deep Sea
869 Research Part 1: Oceanographic Research Papers 57 (7), 847-859.
870 Bradtmiller, L. I., Anderson, R. F., Fleisher, M. Q., Burckle, L. H., 2006, Diatom productivity
871 in the equatorial Pacific Ocean from the last glacial period to the present: a test of the
872 silicic acid leakage hypothesis. Paleoceanography 21, doi: 10.1029/2006PA001282.
873 -, 2007, Opal burial in the equatorial Atlantic Ocean over the last 30 ka: implicatons for
874 glacial-interglacial changes in the ocean silicon cycle. Paleoceanography 22,
875 doi:10.1029/2007PA001443.
876 -, 2009, Comparing glacial and Holocene opal fluxes in the Pacific sector of the Southern
877 Ocean. Paleoceanography 24, doi:10.1029/2008PA001693.
878 Broecker, W. S., Peng, T.-H., 1987, The role of $CaCO_3$ compensation in the glacial to
879 interglacial atmospheric CO_2 change. Global Biogeochemical Cycles 1, 15-29.
880 Brzezinski, M. A., Dumousseaud, C., Krause, J. W., Measures, C. I., Nelson, D. M., 2008,
881 Iron and silicic acid concentrations together regulate Si uptake in the equatorial
882 Pacific Ocean. Limnology and Oceanography 53, 875-889.
883 Brzezinski, M. A., Nelson, D. M., 1996, Chronic substrate limitation of silicic acid uptake
884 rates in the western Sargasso Sea. Deep-Sea Research II 43, 437-453.
885 Brzezinski, M. A., Sigman, D. M., Sarmiento, J. L., Matsumoto, K., Gruber, N., Rau, G. H.,
886 Coale, K. H., 2002, A switch from $Si(OH)_4$ to NO_3^- depletion in the glacial Southern
887 Ocean. Geophysical Research Letters, 29, 1564.
888 Burke, A., Robinson, L. F., 2011, The Southern Ocean's role in carbon exchange during the

889 last deglaciation. Science 335 (6068), 557-561.
890 Calvo, E., Pelejaro, C., Logan, G. A., Deckker, P., 2004, Dust-induced changes in
891 phytoplankton composition in the Tasman Sea during the last four interglacials.
892 Paleoceanography 19, PA2020.
893 Calvo, E., Pelejero, C., Pena, L. D., Cacho, I., Logan, G. A., 2011, Eastern Equatorial Pacific
894 productivity and related-CO2 changes since the last glacial period. Proceedings of the
895 National Academy of Sciences of the USA 108, 5537-5541.
896 Cao, Z., Frank, M., Dai, M., Grasse, P., Ehlert, C., 2012, Silicon isotope constraints on
897 sources and utilization of silicic acid in the northern South China Sea. Geochimica et
898 Cosmochimica Acta 97, 88-104.
899 Cardinal, D., Alleman, L. Y., Dehairs, F., Savoye, N., Trull, T. W., Andre, L., 2005, Relevance
900 of silicon isotopes to Si-nutrient utilization and Si-source assessment in Antarctic
901 waters. Global Biogeochemical Cycles 19, doi:10.1029/2004GB002364.
902 Cardinal, D., Savoye, N., Trull, T. W., Dehairs, F., E.E., K., Fripiat, F., Tison, J.-L.,André, L.,
903 2007, Silicon isotope in spring Southern Ocean diatoms: large zonal changes despite
904 homogeneity among size fractions. Marine Chemistry 106, 46-62.
905 Chase, Z., Anderson, R. F., Fleisher, M. Q., Kubik, P. W., 2002, The influence of particle
906 composition and particle flux on the scavenging of Th, Pa and Be in the ocean. Earth
907 and Planetary Science Letters 204, 215-229.
908 -, 2003a, Accumulation of biogenic and lithogenic material in the Pacific sector of the
909 Southern Ocean during the past 40,000 years. Deep-Sea Research II 50, 799-832.
910 -, 2003b, Scavenging of Th-230, Pa-231 and Be-10 in the Southern Ocean (SW Pacific
911 Sector): the importance of particle flux, particle composition and advection. Deep-Sea
912 Research II: Topical Studies in Oceanography 50, 739-768.
913 Cortese, G., Gersonde, R., Hillendbrand, C.-D., Kuhn, G., 2004, Opal sedimentation shifts in
914 the World Ocean over the last 15 Myr. Earth and Planetary Science Letters 224, 509-
915 527.
916 Crosta, X., Beucher, C., Pahnke, K., Brzezinski, M. A., 2007, Silicic acid leakge from the
917 Southern Ocean: opposing effects of nutrient uptake and oceanic circulation.
918 Geophysical Research Letters 34, L13601, doi:13610.13029/12006GL029083.
919 De La Rocha, C., Bickle, M., 2005, Sensitivity of silicon isotopes to whole-ocean changes in
920 the silica cycle. Marine Geology 217, 267-282.
921 De La Rocha, C., Brzezinski, M. A., DeNiro, M. J., 1997, Fractionation of silicon isotopes by
922 marine diatoms during biogenic silica formation. Geochimica Cosmochimica Acta 61,
923 5051-5056.
924 De La Rocha, C., Brzezinski, M. A., DeNiro, M. J., Shemesh, A., 1998, Silicon isotope
925 composition of diatoms as an indicator of past oceanic change. Nature 395, 680-683.
926 De La Rocha, C. L., 2003, Silicon isotope fractionation by marine sponges and the
927 reconstruction of the silicon isotope composition of ancient deep water. Geology 31,
928 423-426.
929 De La Rocha, C. L., Bescont, P., Croguennoc, A., Ponzevera, E., 2011, The silicon isotope
930 composition of surface waters in the Atlantic and Indian Sectors of the Southern
931 Ocean. Geochimica et Cosmochimica Acta 75 (18), 5283-5295.
932 De La Rocha, C. L., Brzezinski, M. A., DeNiro, M. J., 2000, A first look at the distribution of
933 the stable isotopes of silicon in natural waters. Geochimica et Cosmochimica Acta 64,
934 2467-2477.
935 de Souza, G. F., Reynolds, B. C., Johnson, G. C., Bullister, J. L., Bourdon, B., 2012a, Silicon
936 stable isotope distribution traces Southern Ocean export of Si to the eastern South
937 Pacific thermocline. Biogeosciences 9, 4199-4213.

de Souza, G. F., Reynolds, B. C., Rickli, J., Frank, M., Saito, M. A., Gerringa, L. J. A., Bourdon, B., 2012b, Southern Ocean control of silicon stable isotope distribution in the deep Atlantic Ocean. Global Biogeochemical Cycles 26 (2), doi:10.1029/2011GB004141.
Demarest, M. S., Brzezinski, M. A., Beucher, C., 2009, Fractionation of silicon isotopes during biogenic silica dissolution. Geochimica et Cosmochimica Acta 73, 5572-5583.
DeMaster, D. J., 2002, The accumulation and cycling of biogenic silica in the Southern Ocean: revisiting the marine silica budget. Deep-Sea Research II 49, 3155-3167.
dos Santos, R. A. L., Wilkins, D., De Deckker, P., Schouten, S., 2012, Late Quaternary productivity changes from offshore Southeastern Australia: A biomarker approach. Palaeogeography Palaeoclimatology Palaeoecology 363, 48-56.
Dubois, N., Kienast, M., Kienast, S., Calvert, S. E., Francois, R., Anderson, R. F., 2010, Sedimentary opal records in the eastern equatorial Pacific: it's not all about leakage. Global Biogeochemical Cycles 24, GB4020, doi:4010.1029/2010GC003821.
Egan, K., Rickaby, R. E. M., Leng, M. J., Hendry, K. R., Hermoso, M., Sloane, H. J., Bostock, H., Halliday, A. N., 2012, Diatom silicon isotopes as a proxy for silicic acid utilisation: A Southern Ocean core top calibration. Geochimica et Cosmochimica Acta 96, 174-192.
Ehlert, C., Grasse, P., Frank, M., 2013, Changes in silicate utilisation and upwelling intensity off Peru since the Last Glacial Maximum - insights from silicon and beodymium isotopes. Quaternary Science Reviews 72, 18-35.
Ellwood, M. J., Hunter, K. A., 1999, Determination of the Zn/Si ratio in diatom opal: a method for the separation, cleaning and dissolution of diatoms. Marine Chemistry 66, 149-160.
Ellwood, M. J., Wille, M., Maher, W., 2010, Glacial silicic acid concentrations in the Southern Ocean. Science 330, 1088-1091.
Etourneau, J., Ehlert, C., Frank, M., Martinez, P., Schneider, R., 2012, Contribution of changes in opal productivity and nutrient distribution in the coastal upwelling systems to Late Pliocene/Early Pleistocene climate cooling. Climate of the Past 8, 1435-1445.
Falkowski, P. G., Katz, M. E., Knoll, A. H., Quigg, A., Raven, J. A., Schofield, O., Taylor, F. J. R., 2004, The evolution of modern eukaryotic phytoplankton. Science 305, 354-360.
Frank, N., Gersonde, R., Rutgers van der Loeff, M. M., Bohrmann, G., Nürnberg, C. C., Kubik, P. W., Suter, M., Mangini, A., 2000, Similar glacial and interglacial export productivity in the Atlantic sector of the Southern Ocean. Multiproxy evidence and implications for glacial atmospheric CO_2. Paleoceanography 15, 642-658.
Fripiat, F., Cardinal, D., Tison, J.-L., Worby, A., André, L., 2007, Diatom-induced silicon isotopic fractionation in Antarctic sea ice. Journal of Geophysical Research 112, doi:10.1029/2006JG000244.
Fripiat, F., Cavagna, A.-J., Dehairs, F., de Brauwere, A., Andre, L., Cardinal, D., 2012, Processes controlling the Si-isotopic composition in the Southern Ocean ad application for paleoceanography. Biogeosciences 9, 2443-2457.
Fripiat, F., Cavagna, A.-J., Savoye, N., Dehairs, F., Andre, L., Cardinal, D., 2011, Isotopic constraints on the Si-biogeochemical cycle of the Antarctic Zone in the Kerguelen area (KEOPS). Marine Chemistry 123 (1-4), 11-22.
Froelich, P. N., Blanc, V., Mortlock, R. A., Chillrud, S. N., 1992, River fluxes of dissolved silica to the ocean were higher during glacials. Ge/Si in diatoms, rivers and oceans: Paleoceanography 7, 739-767.
Georg, R. B., West, A. J., Basu, A. R., Halliday, A. N., 2009, Silicon fluxes and isotope

composition of direct groundwater discharge into the Bay of Bengal and the effect on the global ocean silicon budget. Earth and Planetary Science Letters 283 (1-4), 67-74.
Griffiths, J. D., Barker, S., Hendry, K. R., Thornalley, D. J. R., van de Flierdt, T., Hall, I. R., Anderson, R. F., 2013, Evidence of silicic acid leakage to the tropical Atlantic via Antarctic Intermediate Water during marine isotope stage 4. Paleoceanography 28, 307-318.
Gutjahr, M., Frank, M., Stirling, C. H., Keigwin, L. D., Halliday, A. N., 2008, Tracing the Nd isotope evolution of North Atlantic deep and intermediate waters in the western North Atlantic since the Last Glacial Maximum from Blake Ridge sediments: Earth and Planetary Science Letters 266 (1-2), 61-77.
Harrison, K. G., 2000, Role of increased marine silica input on paleo-pCO2 levels. Paleoceanography 15, 292-298.
Hayes, C. T., Anderson, R. F., Fleisher, M. Q., 2011, Opal accumulaiton rates in the equatorial Pacific and mechanisms of deglaciation. Paleoceanography 26, PA1207, doi:1210.1029/2010PA002008.
Hendry, K. R., Andersen, M. B., 2013, The zinc isotopic composition of siliceous marine sponges: investigating nature's sediment traps. Chemical Geology 354, 33-41.
Hendry, K. R., Georg, R. B., Rickaby, R. E. M., Robinson, L. F., Halliday, A. N., 2010, Deep ocean nutrients during the Last Glacial Maximum deduced from sponge silicon isotopic compositions. Earth and Planetary Science Letters 292, 290-300.
Hendry, K. R., Leng, M. J., Robinson, L. F., Sloane, H. J., Blusztjan, J., Rickaby, R. E. M., Georg, R. B., Halliday, A. N., 2011, Silicon isotopes in Antarctic sponges: an interlaboratory comparison. Antarctic Science 23, 34-42.
Hendry, K. R., Rickaby, R. E. M., 2008, Opal (Zn/Si) ratios as a nearshore geochemical proxy in coastal Antarctica. Paleoceanography 23, PA2218, doi:10.1029/2007PA001576.
Hendry, K. R., Robinson, L. F., 2012, The relationship between silicon isotope fractionation in sponges and silicic acid concentration: modern and core-top studies of biogenic opal. Geochimica et Cosmochimica Acta 81, 1-12.
Hendry, K. R., Robinson, L. F., McManus, J. F., Hays, J. D., in press, Silicon isotopes indicate enhanced carbon export efficiency in the North Atlantic during deglaciation. Nature Communications.
Hendry, K. R., Robinson, L. F., Meredith, M. P., Mulitza, S., Chiessi, C. M., and Arz, H., 2012, Abrupt changes in high-latitude nutrient supply to the Atlantic during the last glacial cycle: Geology 40 (2), 123-126.
Higginson, M. J., Altabet, M. A., 2004, Initial tests of the silicic acid leakage hypothesis using sedimentary biomarkers: Geophysical Research Letters 31, L18303, doi:18310.11029/12004GL020511.
Holte, J., Talley, L. D., Chereskin, T. K., Sloyan, B.M., 2012, The role of air-sea fluxes in Subantarctic Mode Water formation. Journal of Geophysical Research 117, C03040, doi:10.1029/2011JC007798.
Horn, M. G., Beucher, C., Robinson, R. S., Brzezinski, M. A., 2011, Southern Ocean nitrogen and silicon dynamics during the last deglaciation. Earth and Planetary Science Letters 310, 334-339.
Hutchins, D.A., DiTullio, G.R., Zhang, Y., Bruland, K.W., 1998. An iron limitation mosaic in the California upwelling regime. Limnology and Oceanography 43 (6), 1037-1054.
Jaccard, S. L., Hayes, C. T., Martinez-Garcia, A., Hodell, D. A., Anderson, B. E., 2013, Two modes of change in Southern Ocean productivity over the past million years. Science 339, 1419-1423.
Johnson, H. P., Hautala, S. L., Bjorklund, T. A., Zarnetske, M. R., 2006, Quantifying the

North Pacific silica plume. Geochemistry Geophysics Geosystems 7, Q05011, doi:05010.01029/02005GC001065.
Keigwin, L. D., 2004, Radiocarbon and stable isotope constrainst on Last Glacial Maximum and Younger Dryas ventilation in the western North Atlantic. Paleoceanography 19, PA4012, doi:4010.1029/2004PA001029.
Kemp, A. E. S., Pearce, R. B., Grigorov, I., Rance, J., Lange, C. B., Quilty, P., Salter, I., 2006, Production of giant marine diatoms and their export at oceanic frontal zones: implications for Si and C flux from stratified oceans. Global Biogeochemical Cycles 20, doi: 10.1029/2006GB002698.
Kienast, S. S., Kienast, M., Jaccard, S., Calvert, S. E., Francois, R., 2006, Testing the silica leakage hypothesis with sedimentary opal records from the eastern equatorial Pacific over the last 150 kyrs. Geophysical Research Letters 33, L15607, doi:15610.11029/12006GL026651.
Koutavas, A., Sachs, J. P., 2008, Northern timing of deglaciation in the eastern equatorial Pacific from alkenone paleothermometry. Paleoceanography 23, doi:10.1029/2008PA001593.
Kumar, N., Anderson, R.F., Mortlock, R.A., Froelich, P.N., Kubik, P., Dittrich-Hannen, B., Suter, M., 1995, Increased biological productivity and export production in the glacial Southern Ocean. Nature 378, 675-680.
Lal, D., Charles, C., Vacher, L., Goswami, J. N., Jull, A. J. T., McHargue, L., Finkel, R. C., 2006, Paleo-ocean chemistry records in marine opal: implications for fluxes of trace elements, cosmogenic nuclides (^{10}Be and ^{26}Al), and biological productivity. Geochimica Cosmochimica Acta 70, 3275-3289.
Lambert, F., Delmonte, B., Petit, J.R., Bigler, M., Kaufmann, P.R., Hutterli, M.A., Stocer, T.F., Ruth, U., Steffensen, J.P., Maggi, V., 2008, Dust-climate couplings over the past 800,000 years from the EPICA Dome C ice core. Nature 452, 616-619.
Leng, M. J., Sloane, H. J., 2008, Combined oxygen and silicon isotope analysis of biogenic silica. Journal of Quaternary Science 23, 313-319.
Maldonado, M., Navarro, L., Grasa, A., Gonzalez, A., Vaquerizo, I., 2011, Silicon uptake by sponges: a twist to understanding nutrient cycling on continental margins. Nature Scientific Reports 1, doi:10.1038/srep00030.
Mangini, A., Godoy, J. M., Godoy, M. L., Kowsman, R., Santos, G. M., Ruckelshausen, M., Schroeder-Ritzrau, A., and Wacker, L., 2010, Deep sea corals off Brazil verify a poorly ventilated Southern Pacific Ocean during H1 and the Younger Dryas: Earth and Planetary Science Letters, v. 293, p. 269-276.
Marchetti, A., Harrison, P.J., 2007. Coupled changes in the cell morphology and the elemental (C, N and Si) composition of the pennate diatom *Pseudo-nitzschia* due to iron deficiency. Limnology and Oceanography 52 (5), 2270-2284.
Marinov, I., Gnanadesikan, A., Sarmiento, J. L., Toggweiler, J. R., Follows, M., Mignone, B. K., 2008, Impact of oceanic circulation on biological carbon storage in the ocean and atmospheric pCO2. Global Biogeochemical Cycles 22, GB3007, doi:3010.1029/2007GB002958.
Marinov, I., Gnanadesikan, A., Toggweiler, R., Sarmiento, J. L., 2006, The Southern Ocean biogeochemical divide. Nature 441, 964-968.
Martin-Jezequel, V., Hildebrand, M., Brzezinksi, M. A., 2003, Silicon metabolism in diatoms: Implications for growth, Journal of Phycology 36 (5), 821-840.
Marshall, J., Speer, K., 2012, Closure of the meridional overturning circulation through Southern Ocean upwelling. Nature Geosciences, 5, 171-180.
Matsumoto, K., Sarmiento, J. L., 2008, A corollary to the silicic acid leakage hypothesis.

1085 Paleoceanography 23, doi:10.1029/2007PA001515.
1086 Matsumoto, K., Sarmiento, J. L., Brzezinski, M. A., 2002, Silicic acid leakage from the
1087 Southern Ocean: a possible explanation for glacial atmospheric pCO_2. Global
1088 Biogeochemical Cycles 16, 1031.
1089 McClymont, E. L., Ganeshram, R. S., Pichevin, L. E., Talbot, H. M., van Dongen, B. E.,
1090 Thunell, R. C., Haywood, A. M., Singarayer, J. S., Valdes, P. J., 2012, Sea-surface
1091 temperature records of Termination I in the Gulf of California: Challenges for
1092 seasonal and interannual analogies of tropical Pacific climate change,
1093 Paleoceanography 27, doi:10.1029/2011PA002226.
1094 McManus, J. F., Francois, R., Gherardi, J.-M., Keigwin, L. D., Brown-Leger, S., 2004,
1095 Collapse and rapid resumption of Atlantic meridional circulation linked to deglacial
1096 climate changes. Nature 428, 834-837.
1097 Meckler, A. N., Sigman, D. M., Gibson, K. A., Francois, R., Martinez-Garcia, A., Jaccard, S.
1098 L., Rohl, U., Peterson, L. C., Tiedemann, R., Haug, G. H., 2013, Deglacial pulses of
1099 deep-ocean silicate into the subtropical North Atlantic Ocean. Nature 495, 495-498.
1100 Milligan, A. J., Varela, D. E., Brzezinski, M. A., Morel, F. M. M., 2004, Dynamics of silicon
1101 metabolism and silicon isotopic discrimination in a marine diatom as a function of
1102 pCO_2. Limnology and Oceanography 49, 322-329.
1103 Minoletti, F., Hermoso, M., Gressier, V., 2009, Separation of sedimentary micron-sized
1104 particles for palaeoceanography and calcareous nannoplankton biogeochemistry.
1105 Nature Protocols 4, 14-24.
1106 Moreno, A., Nave, S., Kuhlmann, H., Canals, M., Targarona, J., Freudenthal, T., Abrantes, F.
1107 G., 2002, Productivity response in the North Canary Basin to climate changes during
1108 the last 250,000 yr: a multi-proxy approach. Earth and Planetary Science Letters 196
1109 (3-4) 147-159.
1110 Nelson, D. M., Anderson, R. F., Barber, R. T., Brzezinski, M. A., Buesseler, K. O., Chase, Z.,
1111 Collier, R. W., Dickson, M.-L., Francois, R., Hiscock, M. R., Honjo, S., Marra, J.,
1112 Martin, W. R., Sambrotto, R. N., Sayles, F. L., Sigman, D. E., 2002, Vertical budgets
1113 for organic carbon and biogenic silica in the Pacific sector of the Southern Ocean,
1114 1996-1998. Deep-Sea Research II 49, 1645-1674.
1115 Nelson, D. M., Treguer, P., Brzezinski, M. A., Leynaert, A., Queguiner, B., 1995, Production
1116 and dissolution of biogenic silica in the ocean: revised global estimates, comparison
1117 with regional data and relationship to biogenic sedimentation. Global Biogeochemical
1118 Cycles 9, 359-372.
1119 Nozaki, Y., Yamamoto, Y., 2001, Radium 228 based nitrate fluxes in the eastern Indian Ocean
1120 and the South China Sea and silica-induced "alkalinity pump" hypothesis. Global
1121 Biogeochemical Cycles 15, 555-567.
1122 Opfergelt, S., Burton, K. W., Pogge von Strandmann, P. A. E., Gislason, S. R., Halliday, A.
1123 N., 2013, Riverine silicon isotope variations in glaciated basaltic terrains: Implications
1124 for the Si delivery to the ocean over glacial-interglacial intervals. Earth and Planetary
1125 Science Letters 369-370, 211-219.
1126 Pahnke, K., Zahn, R., 2005, Southern Hemisphere water mass conversion linked with North
1127 Atlantic climate variability. Science 307, 1741-1746.
1128 Pahnke, K., Goldstein, S. L., Hemming, S. R., 2008, Abrupt changes in Antarctic Intermediate
1129 Water circulation over the past 25,000 years. Nature Geoscience 1, 870-874.
1130 Pena, L., Goldstein, S. L., Hemming, S. R., Jones, K. M., Calvo, E., Pelejero, C., Cacho, I.,
1131 2013, Rapid changes in meridional advection of Southern Ocean intermediate waters
1132 to the tropical Pacific during the last 30 kyr. Earth and Planetary Science Letters 368,
1133 20-32.

Pichat, S., Sims, K. W. W., Francois, R., McManus, J. F., Leger, S. B., Albarede, F., 2004, Lower export production during glacial periods in the equatorial Pacific from $(^{231}Pa/^{230}Th)_{xs,0}$ measurements in deep-sea sediments. Paleoceanography 19, PA4023, doi:4010.1029/2003PA000994.

Pichevin, L. E., Ganeshram, R. S., Francavilla, S., Arellano-Torres, E., Pedersen, T. F., Beaufort, L., 2010, Interhemispheric leakage of isotopically heavy nitrate in the eastern tropical Pacific during the last glacial period. Paleoceanography 25, PA1204, doi:1210.1029/2009PA001754.

Pichevin, L. E., Reynolds, B. C., Ganeshram, R. S., Cacho, I., Pena, L., Keefe, K., Ellam, R. M., 2009, Enhanced carbon pump inferred from relaxation of nutrient limitation in the glacial ocean. Nature 459, 1114-1117.

Piotrowski, A. M., Goldstein, S. L., Hemming, S. R., Fairbanks, R. G., Zylberberg, D. R., 2008, Oscillating glacial northern and southern deep water formation from combined neodymium and carbon isotopes: Earth and Planetary Science Letters 272, 394-405.

Pondaven, P., Ragueneau, O., Tréguer, P., Hauvespre, A., Dezileau, L., Reyss, J. L., 2000, Resolving the "opal paradox" in the Southern Ocean. Nature 405, 168-172.

Reincke, T., Barthel, D., 1997, Silica uptake kinetics of *Halichondria panicea* in Kiel Bight. Marine Biology 129, 591-593.

Ren, H., Brunelle, B. G., Sigman, D. M., Robinson, R. S., 2013, Diagenetic aluminium uptake into diatom frustules and the preservation of diatom-bound organic nitrogen. Marine Chemistry 155, 92-102.

Reynolds, B. C., 2009, Modeling the modern marine $\delta^{30}Si$ distribution: Global Biogeochemical Cycles 23, GB2015, doi:2010.1029/2008GB003266.

Reynolds, B. C., Frank, M., and Halliday, A. N., 2006, Silicon fractionation during nutrient utilization in the North Pacific. Earth and Planetary Science Letters 244, 431-443.

Richaud, M., Loubere, P., Pichat, S., Francois, R., 2007, Changes in opal flux and the rain ratio during the last 50,000 years in the equatorial Pacific. Deep-Sea Research II: Topical Studies in Oceanography 54 (5-7), 762-771.

Rickaby, R. E. M., Bard, E., Sonzogni, C., Rostek, F., Beaufort, L., Barker, S., Rees, G., Schrag, D. P., 2007, Coccolith chemistry reveals secular variations in the global ocean carbon cycle? Earth and Planetary Science Letters 253 (1-2), 83-95.

Roberts, N. L., Piotrowski, A. M., McManus, J. F., Keigwin, L. D., 2010, Synchronous deglacial overturning and water mass source changes. Science 327, 75-78.

Robinson, L. F., Adkins, J. F., Keigwin, L. D., Southon, J., Fernandez, D. P., Wang, S.-L., Scheirer, D. S., 2005a, Radiocarbon variability in the western North Atlantic during the last deglaciation. Science 310, 1469-1473.

Robinson, R. S., Brunelle, B. G., Sigman, D. M., 2004, Revisiting nutrient utilization in the glacial Antarctic: evidence from a new method for diatom-bound N isotope analysis: Paleoceanography, v. 19, p. doi:10.1029/2003PA000996.

Robinson, R. S., Sigman, D. M., DiFiore, P. J., Rohde, M. M., Mashiotta, T. A., and Lea, D. W., 2005b, Diatom-bound $^{15}N/^{14}N$: New support for enhanced nutrient consumption in the ice age subantarctic. Paleoceanography 20 (3), doi:10.1029/2004PA001114.

Romero, O. E., 2010, Changes in style and intensity of production in the Southeastern Atlantic over the last 70,000 yr. Marine Micropaleontology 74 (1-2), 15-28.

Romero, O. E., Kim, J.-H., Donner, B., 2008, Submillenial-to-millenial variability of diatom production off Mauritania, NW Africa, during the last glacial cycle. Paleoceanography 23, PA3218, doi:3210.1029/2008PA001601.

Romero, O. E., Leduc, G., Vidal, L., Fischer, G., 2011, Millennial variability and long-term changes of the diatom population in the eastern equatorial Pacific during the last

glacial cycle. Paleoceanography 26, doi:10.1029/2010PA002099.
Sarmiento, J. L., Gruber, N., Brzezinski, M. A., Dunne, J. P., 2004, High-latitude controls of thermocline nutrients and low latitude biological productivity. Nature 427, 56-60.
Shemesh, A., 1989, Late Cenozoic Ge/Si record of marine biogenic opal: implications for variations of riverine fluxes to the ocean. Paleoceanography 4, 221-234.
-, 1995, Late Pleistocene oxygen isotope records of biogenic silica from the Atlantic sector of the Southern Ocean. Paleoceanography 10, 179-196.
Sigman, D. M., Hain, M. P., Haug, G. H., 2010, The polar ocean and glacial cycles in atmospheric CO_2 concentration. Nature 466, 47-55.
Spero, H. J., Lea, D. W., 2002, The cause of carbon isotope minimum events on glacial terminations. Science 296, 522-525.
Sutton, J., Varela, D., Brzezinski, M. A., Beucher, C., 2013, Species-dependent silicon isotope fractionation by marine diatoms. Geochimica et Cosmochimica Acta 104, 300-309.
Takeda, S., 1998. Influence of iron availability on nutrient consumption ratio of diatoms in oceanic waters. Nature 393 (6687), 774-777.
Thornalley, D. J. R., Barker, S., Broecker, W. S., Elderfield, H., McCave, I. N., 2011, The deglacial evolution of North Atlantic deep convection. Science 331 (6014), 202-205.
Toggweiler, R., 1999, Variation of atmospheric CO_2 by ventilation of the ocean's deepest water. Paleoceanography 14, 571-588.
Tréguer, P., De la Rocha, C. L., 2013, The world ocean silica cycle. Annual Review of Marine Science 5, 477-501.
Tréguer, P., Nelson, D. M., Van Bennekom, A. J., DeMaster, D. J., Leynaert, A., Quéguiner, B., 1995, The silica balance in the world ocean: a re-estimate. Science 268, 375-379.
Varela, D. E., Pride, C. J., Brzezinski, M. A., 2004, Biological fractionation of silicon isotopes in Southern Ocean surface waters. Global Biogeochemical Cycles 18, doi:10.1029/2003GB002140.
Vink, A., Ruhlemann, C., Zonneveld, K. A. F., Mulitza, S., Huls, M., Willems, H., 2001, Shifts in the position of the North Equatorial Current and rapid productivity changes in the western Tropical Atlantic during the last glacial. Paleoceanography 16 (5), 479-490.
Wetzel, F., de Souza, G.F., Reynolds, B.C., in review, Silicon isotope effects during diatom dissolution and their sensitivity to sample composition: Geochimica Cosmochimica Acta.
Wille, M., Sutton, J., Ellwood, M. J., Sambridge, M., Maher, W., Eggins, S., Kelly, M., 2010, Silicon isotopic fractionation in marine sponges: a new model for understanding silicon isotopic fractionation in sponges. Earth and Planetary Science Letters 292, doi:10.1016/j.epsl.2010.1001.1036.
Wischmeyer, A. G., De La Rocha, C., Maier-Raimer, E., Wolf-Gladrow, D. A., 2003, Control mechanisms for the oceanic distribution of silicon isotopes: Global Biogeochemical Cycles, v. 17, p. doi:10.1029/2002GB002022.
Wu, S., Ding, T., Meng, X., Bai, L., 1997, Determinaton and geological implication of O-Si isotope of the sediment core in the CC area, the Pacific Ocean. Chinese Science Bulletin 42, 1462-1465.
Xie, R. C., Marcantonio, F., Schmidt, M. W., 2012, Deglacial variability of Antarctic Intermediate Water penetration into the North Atlantic from authigenic neodymium isotope ratios. Paleoceanography 27 (3) doi:10.1029/2012/PA002337.
Xiong, Z., Li, T., Crosta, X., Algeo, T., Chang, F., Zhai, B., 2013, Potential role of giant

marine diatoms in sequestration of atmsopheric CO_2 during the Last Glacial Maximum: $\delta^{13}C$ evidence from laminated *Ethmodiscus rex* mats in tropical West Pacific. Global and Planetary Change 108, 1-14.

Zhai, B., Li, T., Chang, F., Cao, Z., 2009, Vast laminated diatom mat deposits from the west low-latitude Pacific Ocean in the last glacial period: Chinese Science Bulletin 54 (23), 4529-4533.

Ziegler, K., Chadwick, O. A., Brzezinski, M. A., Kelly, E. F., 2005, Natural variations of $\delta^{30}Si$ ratios during progressive basalt weathering, Hawaiian Islands. Geochimica et Cosmochimica Acta 69 (19), 4597-4610.

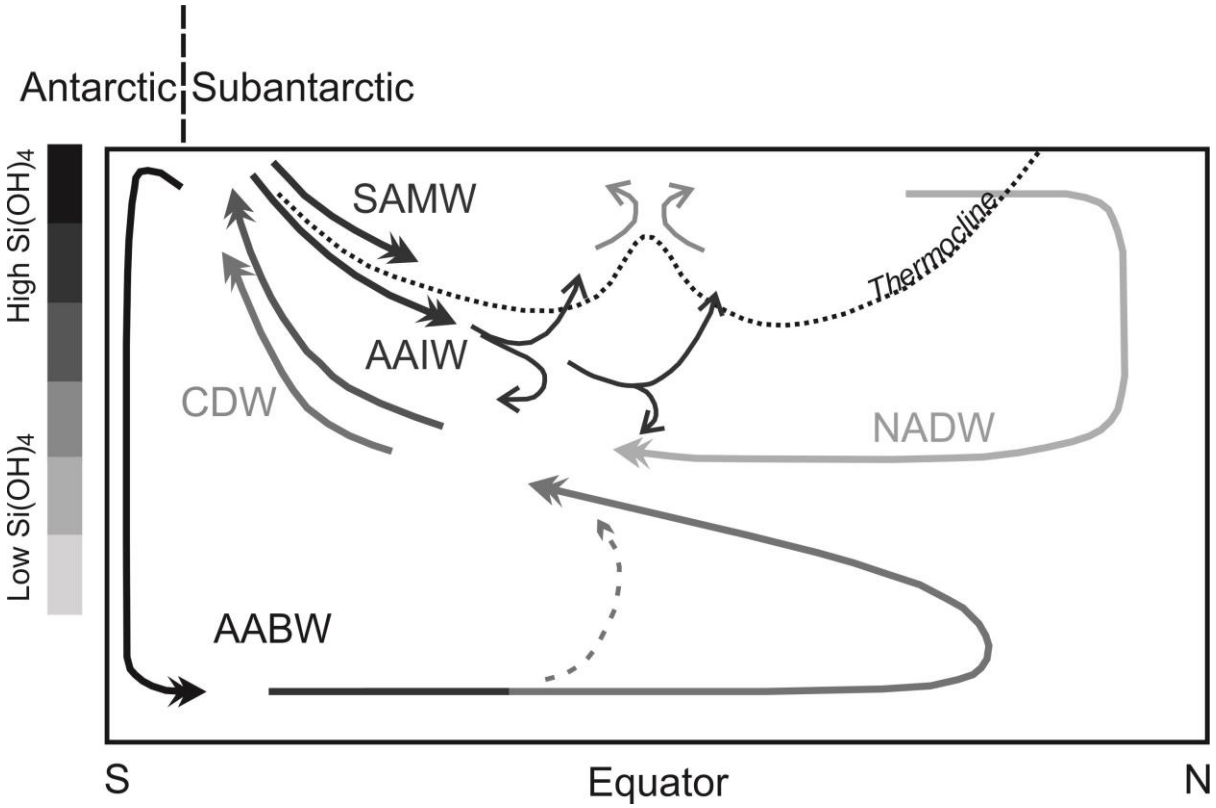

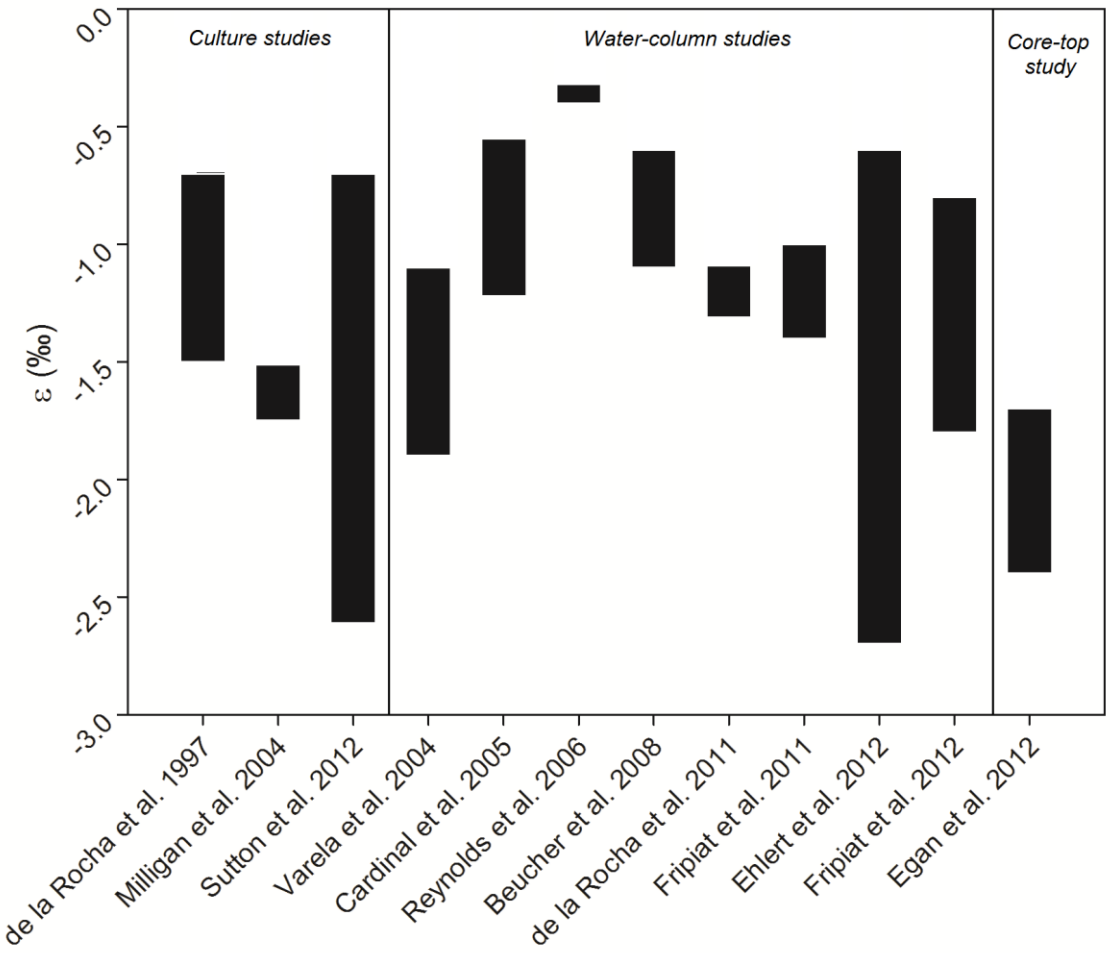
Culture studies
Water-column studies
Core-top study
ε (‰)
0.0
-0.5
-1.0
-1.5
-2.0
-2.5
-3.0
de la Rocha et al. 1997
Milligan et al. 2004
Sutton et al. 2012
Varela et al. 2004
Cardinal et al. 2005
Reynolds et al. 2006
Beucher et al. 2008
de la Rocha et al. 2011
Fripiat et al. 2011
Ehlert et al. 2012
Fripiat et al. 2012
Egan et al. 2012

1242

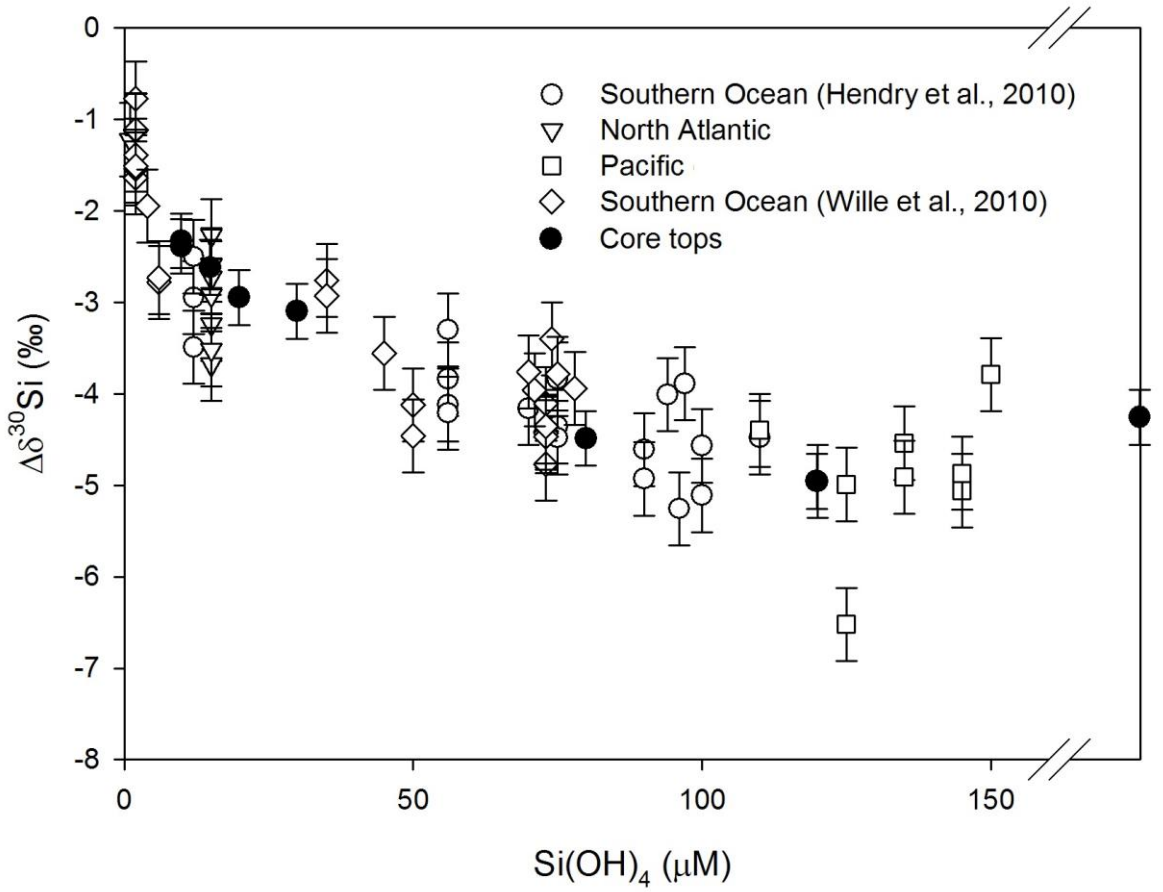
Southern Ocean (Hendry et al., 2010)
North Atlantic
Pacific
Southern Ocean (Wille et al., 2010)
Core tops
$\Delta\delta^{30}Si$ (‰)
$Si(OH)_4$ (μM)
0
-1
-2
-3
-4
-5
-6
-7
-8
0
50
100
150

1243

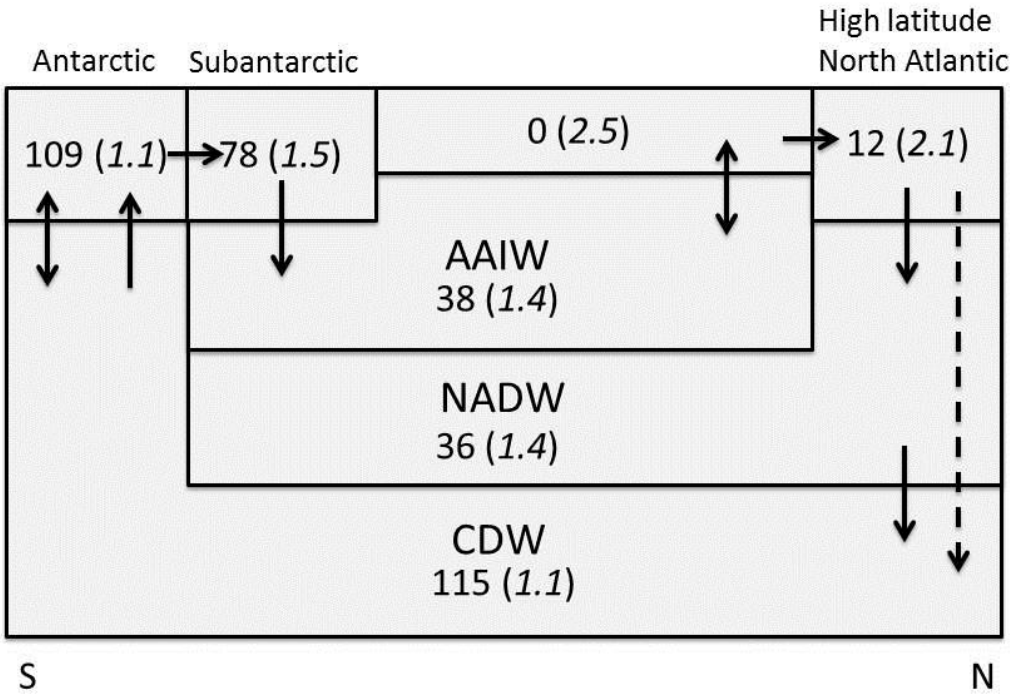
Antarctic
Subantarctic
High latitude
North Atlantic
109 (1.1)
78 (1.5)
0 (2.5)
12 (2.1)
AAIW
38 (1.4)
NADW
36 (1.4)
CDW
115 (1.1)
S
N

1244

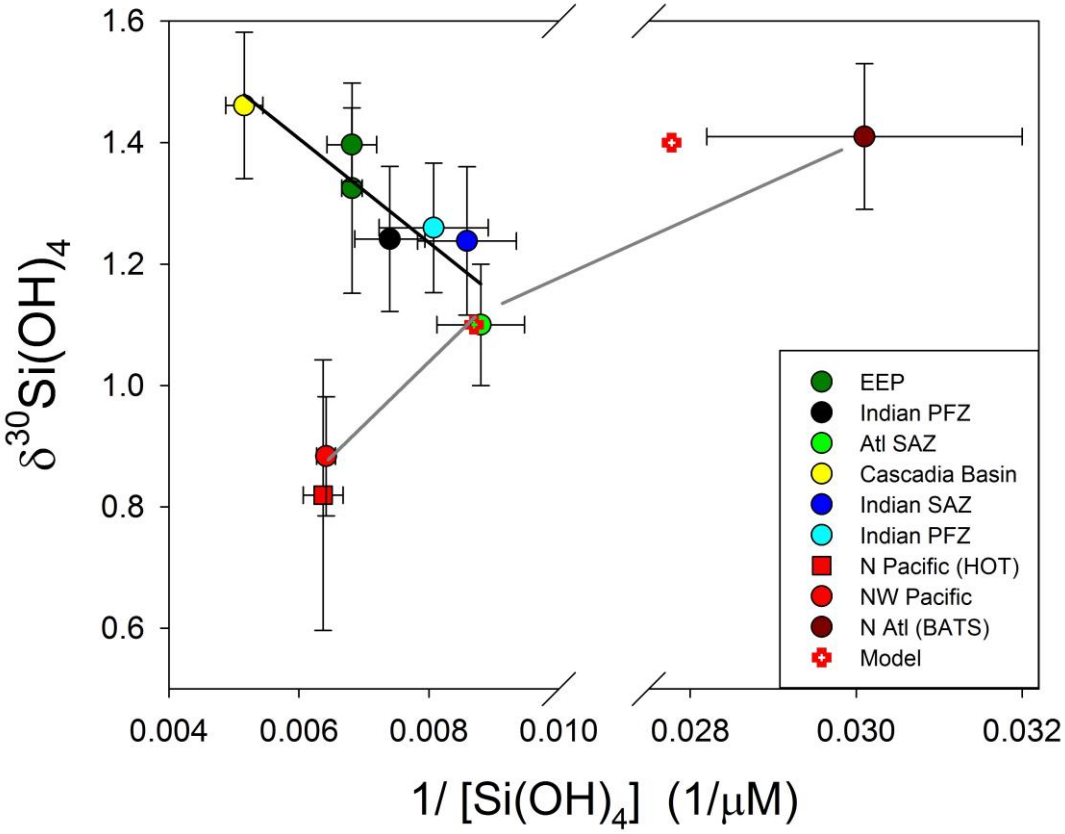
1.6
1.4
1.2
1.0
0.8
0.6
δ30Si(OH)4
0.004
0.006
0.008
0.010
0.028
0.030
0.032
1/ [Si(OH)4] (1/μM)
EEP
Indian PFZ
Atl SAZ
Cascadia Basin
Indian SAZ
Indian PFZ
N Pacific (HOT)
NW Pacific
N Atl (BATS)
Model

1245

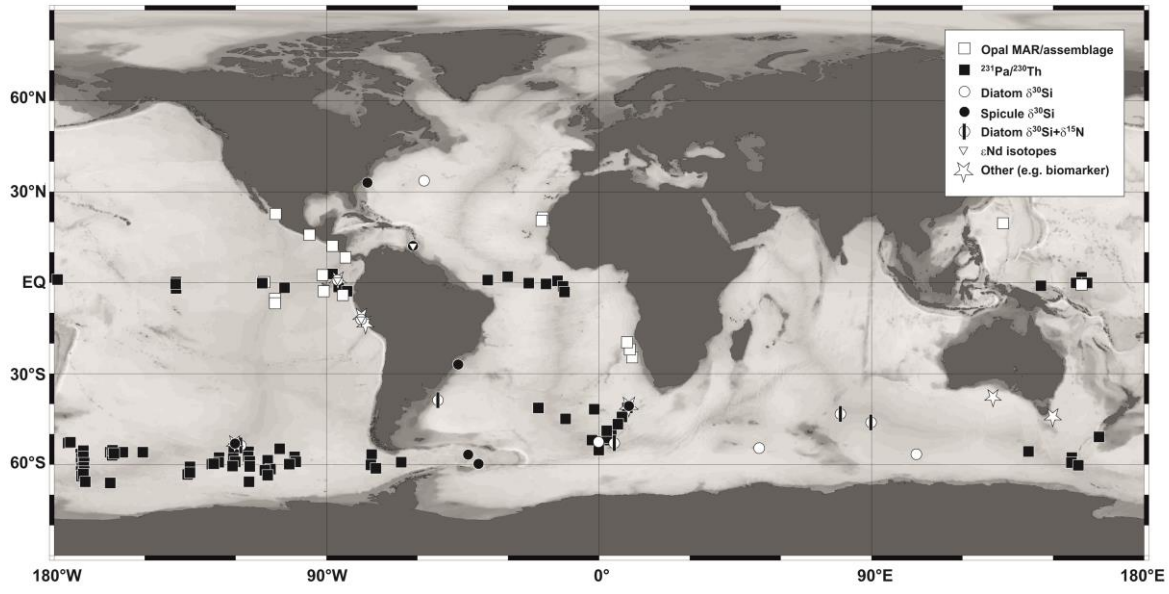
Opal MAR/assemblage
231Pa/230Th
Diatom δ30Si
Spicule δ30Si
Diatom δ30Si+δ15N
εNd isotopes
Other (e.g. biomarker)
60°N
30°N
EQ
30°S
60°S
180°W
90°W
0°
90°E
180°E

1246

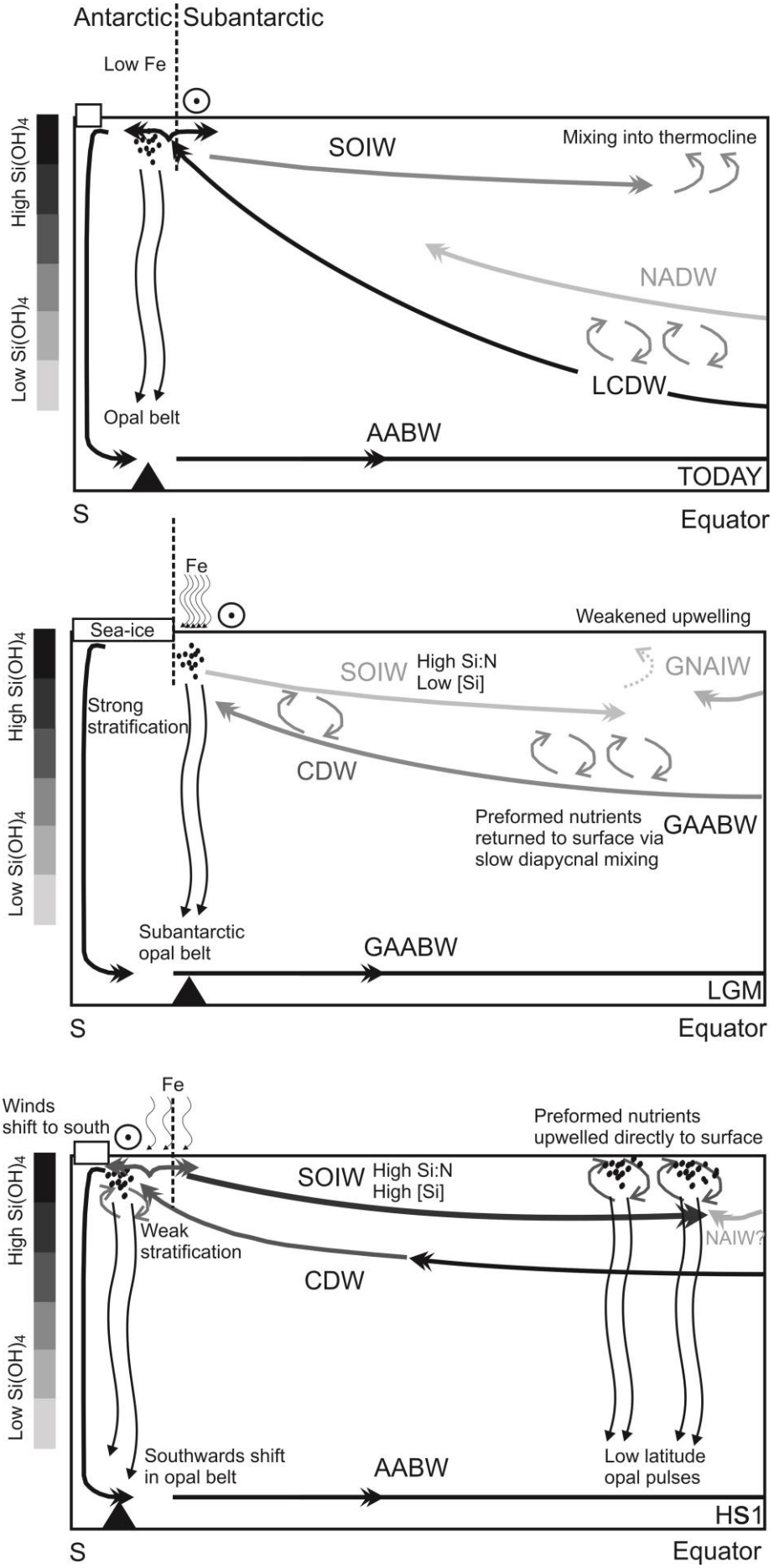
Antarctic
Subantarctic
Low Fe
High Si(OH)4
Low Si(OH)4
SOIW
Mixing into thermocline
NADW
LCDW
Opal belt
AABW
TODAY
S
Equator
Fe
Sea-ice
Weakened upwelling
SOIW
High Si:N
Low [Si]
GNAIW
Strong
stratification
CDW
Preformed nutrients
returned to surface via
slow diapycnal mixing
GAABW
Subantarctic
opal belt
GAABW
LGM
S
Equator
Fe
Winds
shift to south
Preformed nutrients
upwelled directly to surface
SOIW
High Si:N
High [Si]
Weak
stratification
NAIW?
CDW
Southwards shift
in opal belt
AABW
Low latitude
opal pulses
HS1
S
Equator

1247